2017

Biotic interchange has structured Western Hemisphere mammal communities

Danielle Fraser

S. Kathleen Lyons

Running title: Western hemisphere mammal community structure

BIOTIC INTERCHANGE HAS STRUCTURED WESTERN HEMISPHERE MAMMAL COMMUNITIES

Authors: Danielle Fraser[1,2], S. Kathleen Lyons[2,3]

Affiliations: [1]Palaeobiology, Canadian Museum of Nature, PO Box 3443 Stn "D", Ottawa, ON Canada K1P 6P4

[2]Department of Paleobiology, Smithsonian Institution, National Museum of Natural History, 10th and Constitution NW, Washington, DC 20560-0121

[3]School of Biological Sciences, University of Nebraska Lincoln, Lincoln, NE 68588

Emails: Danielle Fraser, DFraser@mus-nature.ca; S. Kathleen Lyons, katelyons@unl.edu

Corresponding author: Danielle Fraser

Keywords: Biotic interchange, competition, climate filtering, limiting similarity, body mass dispersion, tropics, mammals, Net Relatedness Index, Checkerboard scores, latitudinal gradient

Abstract words: 298

Body words: 6,351

References: 107

Abstract

Aim.— Many hypotheses posit that species-rich tropical communities are dominated by species-species interactions, apparent as competitive exclusion or character displacement, whereas species-poor temperate communities are dominated by species-environment interactions. Recent studies demonstrate a strong influence of macroevolutionary and biogeographic factors. We simultaneously test for the effects of species interactions, climate, and biotic interchange on Western Hemisphere mammal communities using a phylogenetic and functional diversity approach.

Location.— Western Hemisphere.

Time period.— Modern

Major taxa studied.— Mammalia

Methods.— Using Western Hemisphere mammal distributional and body mass data, we calculate body mass dispersion, phylogenetic diversity (Net Relatedness Index), and assemblage-averaged rates of co-occurrence (Checkerboard scores) in 100 km by 100 km grid cells under an equal area projection. We model body mass dispersion as a function of phylogenetic diversity, co-occurrence rates, and species richness, as well as mean annual temperature and precipitation. We infer rates of dispersal among the temperate and tropical zones of the Western Hemisphere using phylogenetic methods.

Results.— The dispersion of Northern Temperate mammal body masses is higher than null communities and shows correlated change with climate, consistent with resource competition and environmental filtering. Conversely, the dispersion of tropical and Southern Temperate mammal body masses are lower than and not differentiable from null expectations, respectively, suggesting a limited role of species-species and species-environment interactions at the grain of

our analysis. Low tropical body mass dispersion and phylogenetic evenness are best explained by the high rates of faunal mixing. High rates of dispersal might also explain the similarity in community structure between the Southern temperate and tropical zones.

Main Conclusions.— Mammal community assembly processes differ among the temperate and tropical zones of the Western Hemisphere and faunal mixture during dispersal events such as the Great American Biotic Interchange (Pliocene ~3 Ma) may have been important in structuring Western Hemisphere mammal communities.

Introduction

Latitudinal richness gradients (i.e. the decline in species numbers from the tropics to the poles) are nearly ubiquitous, having been observed for many terrestrial and marine organisms in both the present and the past (Brown, 1984; Currie, 1991; Willig & Lyons, 1998; Lyons & Willig, 1999, 2002; Hawkins *et al.*, 2003; Rose *et al.*, 2011; Fraser *et al.*, 2014; Mannion *et al.*, 2014; Marcot *et al.*, 2016). The numerous hypotheses proposed to explain the formation of latitudinal diversity gradients typically posit differences in the primary drivers of community assembly between the species-rich tropical and, comparatively species-poor, temperate regions of the world (Willig *et al.*, 2003; Mittelbach *et al.*, 2007; Belmaker & Jetz, 2015). Species-environment (i.e., environmental filters or energy availability constraints) (Hawkins *et al.*, 2003), species-species (i.e., competition or ecological constraints on coexistence) (Connor & Simberloff, 1979; Mittelbach *et al.*, 2007; Martin & Pfennig, 2009; Lamanna *et al.*, 2014), macroevolutionary (i.e., differences in speciation and extinction rates) (Jablonski *et al.*, 2006; Weir & Schluter, 2007; Condamine *et al.*, 2012; Rolland *et al.*, 2014; Weir, 2014), and historical (i.e., regional differences in area and age) (Rosenzweig, 1995; Fine & Ree, 2006; Jetz & Fine, 2012) effects on community assembly are commonly invoked to explain differences in species richness amongst temperate and tropical zones.

Classical niche theory predicts that differences in the ways species share niche space amongst assemblages reflect differences in community assembly mechanisms (MacArthur & Levins, 1967). Disentangling the relative roles of environmental, ecological, and historical drivers on community assembly therefore requires the comparison of species niche occupation within and among regions that we believe impart particularly strong ecological and

environmental pressures or have differed markedly in the historical processes responsible for populating the regional species pool. Many studies of latitudinal diversity gradients rely on species counts as the variable of interest. Unfortunately, species counts cannot reveal the relative roles of species-environment and species-species interactions nor historical contingencies in community assembly (Safi *et al.*, 2011; Lamanna *et al.*, 2014). However, the advent of methods for quantifying the phylogenetic and functional diversity of species assemblages is enabling ecologists to more directly test for differences in community assembly among regions (Mittelbach *et al.*, 2007; Cantalapiedra *et al.*, 2014; Lamanna *et al.*, 2014; Rolland *et al.*, 2014). In particular, comparing and contrasting evolutionary and trait distances among species in different assemblages is leading to a more thorough understanding of the differences in the drivers of community assembly amongst latitudes (Cadotte *et al.*, 2013).

Environmental filtering, a classical species-environment interaction, is a process whereby species are sorted along abiotic gradients according to their environmental tolerances. Under a strong environmental filter, such as a latitudinal or altitudinal climate gradient, species may meet the limits of their environmental tolerances and be excluded from communities (Hawkins *et al.*, 2003; Soininen *et al.*, 2007a; Soininen, 2010). Species in the same assemblage may therefore share environmental tolerances and show strong trait similarity (MacArthur & Levins, 1967; Soininen *et al.*, 2007b; Cavender-Bares *et al.*, 2009; Lamanna *et al.*, 2014). Furthermore, if traits linked to environmental tolerance show strong phylogenetic signal (i.e., a strong correlation between phylogenetic distances and trait values), both phylogenetic and trait distances should be small for species in the same assemblage (Qian *et al.*, 2013; Cantalapiedra *et al.*, 2014).

Competition involves strong inter- or intraspecific interactions, typically for access to resources (Schoener, 1974). Competition for resources may be most intense when closely related

species in an assemblage share traits (e.g. body size or diet), potentially lowering the fitness of populations from one or both species (Webb *et al.*, 2002; Wiens & Graham, 2005; Ricklefs, 2010). As a result, species may undergo either character displacement or competitive exclusion (via limiting similarity) to reduce the intensity of competition (Mayfield & Levine, 2010). The outcomes of both character displacement and competitive exclusion via limiting similarity are reduced niche overlap amongst co-existing species. However, the latter may also lead to the spatial segregation of closely related species and thus coexistence of phylogenetically distantly related taxa (Schoener, 1974; Connor & Simberloff, 1979; Damuth, 1981; Brown, 1984; Cavender-Bares *et al.*, 2006; Cavender-Bares *et al.*, 2009; Mayfield & Levine, 2010). Alternatively, if habitat preferences and competitiveness (i.e., the ability to exploit resources) show strong phylogenetic signal, competitive exclusion may lead to coexistence of phylogenetically closely related taxa (Mayfield & Levine, 2010).

Historical processes (i.e., macroevolution and dispersal or biotic interchange) are those that determine how many and which types of species are present in a regional pool and available to colonize local communities (Weir & Schluter, 2007; Morales-Castilla *et al.*, 2012; Cantalapiedra *et al.*, 2014; Rolland *et al.*, 2015). Incipient speciation with low rates of dispersal into adjacent regions can lead to high rates of dissimilarity among regional faunas and, if rates of species formation differ sufficiently, large differences in species richness (Ricklefs, 1987; Mittelbach *et al.*, 2007; Weir & Schluter, 2007; McPeek, 2008; Buckley *et al.*, 2010; Cardillo, 2011; Weir, 2014; Fine, 2015; Oliveira *et al.*, 2016). Similarly, imbalance in rates of extinction among clades can lead to large regional differences in richness and niche packing (Johnson, 2002; Razafindratsima *et al.*, 2012; Faurby & Svenning, 2015; Fraser *et al.*, 2015; Lyons *et al.*, 2016).

Dispersal is a process by which individuals of a species colonize new areas. Rates of dispersal and dispersal ability are dependent on the environmental tolerances of species and associated with population-level characteristics such as rates of birth and death (Jocque *et al.*, 2010; Baselga *et al.*, 2012; Dobrovolski *et al.*, 2012). Biogeographic factors such as physical distance and regional connectivity also influence the likelihood of dispersal amongst regions (Bacon *et al.*, 2015). At large spatial scales, faunal mixing as a result of interchange may influence the intensity of competitive interactions, filling of trait space, and, in turn, rates of speciation and extinction (Ricklefs, 2010; Green *et al.*, 2011; Hunt, 2013). Such biotic interchange has occurred numerous times throughout the history of life (Jablonski, 1993; Vermeij, 2005; Jablonski *et al.*, 2013) and is likely a major contributor to differences in community assembly amongst biogeographic regions globally (Baselga *et al.*, 2012; Morales-Castilla *et al.*, 2012; Cantalapiedra *et al.*, 2014).

Herein, we use a functional and phylogenetic diversity framework to test for the differential influence of species-species interactions, species-environment interactions, and historical biotic interchange on mammal community assembly in the tropical and temperate zones of the Western Hemisphere. We quantify the phylogenetic and trait distances of Western Hemisphere mammal assemblages (defined as species whose ranges overlap with the center of 100 km x 100 km grid cells) using body size dispersion (i.e., mean pairwise differences in ln transformed body mass; BM_{dist}) (Fritz & Purvis, 2010) and phylogenetic assemblage structure (i.e., Net Relatedness Index, NRI or standardized mean pairwise phylogenetic distances) (Webb *et al.*, 2002). High values of BM_{dist} indicate reduced niche similarity among coexisting species (evenness) while low values indicate niche overlap (clustering). Similarly, high values of NRI

indicate the coexistence of phylogenetically distantly-related species (phylogenetic evenness) and low values, coexistence of phylogenetically closely-related species (phylogenetic clustering).

Body mass dispersion has been used elsewhere as a measure of functional diversity (Fritz & Purvis, 2010). We use body mass as the functional trait of interest because mammalian body size is a determinant of many niche characteristics including *inter alia* geographic range size, population density, dispersal ability, life history, metabolism, and the thermal niche (Peters, 1983). Furthermore, body mass is collinear with many of the additional traits (e.g., diet) included in the calculation of functional diversity (Pineda-Munoz *et al.*, 2016). As a result, studies that include additional functional variables such as broad dietary category diet (e.g., herbivore, carnivore) do not yield spatial patterns of functional diversity different from those expected for body mass dispersion alone (e.g., functional clustering in the tropics) (Safi *et al.*, 2011; Oliveira *et al.*, 2016; Mazel *et al.*, 2017), suggesting that body mass does capture the major axes of niche variation (Rowan *et al.*, 2016). Body mass is also a highly heritable trait among mammals (Smith *et al.*, 2004) and therefore shows significant phylogenetic signal (Fig. 1A).

To infer rates of faunal mixing, we use assemblage-averaged species co-occurrence rates (i.e., Checkerboard Scores or C-scores) and reconstruct rates of historical dispersal among the tropical and temperate biogeographic zones of the Western Hemisphere (Ree *et al.*, 2005; Ree & Smith, 2008; Matzke, 2013; Matzke, 2014, 2016). C-scores have previously only been tabulated for pairs of species in a series of assemblages (Stone & Roberts, 1990; Gotelli, 2000). Herein, we average the C-scores at the assemblage scale because average values should, for example, reveal regions of range overlap for species that otherwise do not co-occur (i.e., regions of faunal mixing).

We assess three major groups of assembly hypotheses including environmental filtering, competition, and historical dispersal (also referred to as biotic interchange). The following predictions are summarized in Table 1:

i) Environmental filtering may increasingly constrain the ecological diversity of species assemblages, leading to reduced body mass dispersion and increased NRI relative to null assemblages, in correlation with abiotic factors such as mean annual temperature and precipitation.

ii) Classical niche theory predicts that the strength of competitive interactions is reflected in the division of niche space. Species are driven apart in niche space by both competitive exclusion via limiting similarity and character displacement. Both scenarios predict high body mass dispersion but only limiting similarity predicts low values of the Net Relatedness Index relative to null communities. Conversely, we predict that competitive exclusion resulting from phylogenetic conservation of competitive abilities should lead to both low body mass dispersion and high values of NRI relative to null communities. In all scenarios, species richness should predict the intensity of competitive interactions. We assume that competitive interactions are detectable at the grain of our analysis (10,000 km^2 grid cells). Typically, competitive interactions are thought to play out at relatively small spatial scales. However, support for competitive interactions at the grain of our analysis would provide very strong evidence for their operation at large spatial scales. Nonetheless, we are careful not to interpret a lack of support as evidence against the operation of resource competition (that is, failing to reject a null hypothesis cannot be interpreted as support for the null hypothesis).

iii) Dispersal events such as the Great American Biotic Interchange (~ 3 Ma; as well as those that occurred earlier) involved the asymmetric exchange of species amongst biogeographic zones in the Western Hemisphere. We therefore assume that reconstructed rates of interchange amongst the temperate and tropical zones reflect historical rates of dispersal. Furthermore, regions that have acted as either a biotic sink or source for dispersing species should be comprised of species that have had otherwise distinct evolutionary histories (i.e., they should show phylogenetic evenness or low values of NRI). Because C-scores are highest for spatially segregated species. Regions through which biotic interchange has occurred or is occurring should show the highest assemblage averaged C-scores.

Materials and Methods

We downloaded Digital Distribution Maps of Western Hemisphere non-volant Mammals (Patterson *et al.*, 2007), which represent historical mammal ranges. Such maps are preferable to the IUCN maps for our purposes because they reduce the extent to which our conclusions are contingent on human influences. These data have been used in similar recent studies of Western Hemisphere mammal diversity (Polly *et al.*, 2017). We used the taxonomy of Wilson and Reeder (2005). The dataset included 1366 species after the exclusion of a small number of unreadable or corrupted files. We sampled the ranges of extant Western Hemisphere mammals using a Behrmann equal area projection (Faurby & Svenning, 2015) and 100 km by 100 km grid cells. Smaller grid cell sizes are subject to bias (Hurlbert & Jetz, 2007). We considered grid cells to be occupied by a species if the center of the cell intersected with its geographic range (Safi *et al.*, 2011; Faurby & Svenning, 2015). The result was a species by grid cell occurrence matrix, which we used for all further analyses.

Body Mass Dispersion.—

We downloaded body size data for 1070 western hemisphere mammal species from the PanTHERIA database (Jones *et al.*, 2009). Body masses were ln transformed before further analysis. We tested for phylogenetic signal in ln transformed body masses using the phylogeny of (Fritz *et al.*, 2009) and Pagel's lambda in the phytools R package (Revell, 2013). We used ancestral state reconstruction (contMap in phytools) to visualize the distribution of body masses on the Western Hemisphere mammal phylogenetic tree (Revell, 2013). We did not use ancestral state reconstruction of body mass for any purpose beyond visualization.

Because body size is a strong determinant of many niche axes in mammals and shows strong phylogenetic signal (Fig. 1A) (Peters 1983, Western 1979), we assume that similarity in body mass is indicative of niche overlap and thus potential to compete for resources. Therefore, we used body size dispersion (i.e., the average of all pairwise difference in body mass among co-occurring species) as a metric for average rates of niche overlap (Fritz & Purvis, 2010). We calculated body mass dispersion (BM_{dist}) as the mean of the Euclidean distances or absolute differences between all pairs of species in each grid cell. BM_{dist} is equivalent to other mean pairwise distance metrics.

In the absence of niche-based community assembly processes, communities may be comprised of a random subset of species available to colonize a local community. We compared observed BM_{dist} patterns to two null models due to reviewer concerns regarding null model choice. The first was a set of 100 randomizations per grid cell where species were selected from the sample of Western Hemisphere mammals within each region (i.e., the regional pool was comprised only of species in the same biogeographic zone, i.e., Tropics, Southern Temperate, or Northern Temperate) (Lamanna *et al.*, 2014). Total richness was preserved in each cell but

species occupancy was not. For the second null model, we used the independent swap algorithm of (Gotelli, 2000). Swap algorithms, such as the one used here, start with the original occurrence matrix and involve randomly choosing submatrices with adjacent 1's and 0's then swapping them while retaining the row and column totals (Gotelli, 2000; Gotelli & Entsminger, 2001). We used 100,000 iterations of the independent swap algorithm per randomized occurrence matrix of which we generated 100. We have chosen to focus on the results of the independent swap because null models that maintain both grid cell richness and species occupancy yield the most reasonable rates of both Type I and Type II error (Kembel, 2009). Observed BM_{dist} was compared to the randomized communities using standardized effect sizes calculated as SES = (observed – mean(random)) / sd(random).

Because species at the same trophic level might compete most strongly for resources, we also calculated BM_{dist} for all Western Hemisphere mammals and then separately for herbivores plus omnivores (948 species). Carnivoran diversity is too low in the Western Hemisphere for sufficient analysis.

Phylogenetic Assemblage Structure.—

Using the phylogeny of (Fritz *et al.*, 2009), we calculated the Net Relatedness Index (NRI) for each grid cell in the Western Hemisphere using the picante R package (Webb, 2000; Webb *et al.*, 2002; Kembel *et al.*, 2014). The Net Relatedness Index is the standardized effect size of mean pairwise phylogenetic distances (MPD) among co-occurring species (Webb *et al.*, 2002). We have chosen NRI from among the several available metrics for phylogenetic diversity because it shows less co-linearity with species richness due to explicit incorporation of a null model (Oliveira *et al.*, 2016).

The Net Relatedness Index is calculated as:

$$NRI = -1 * \frac{MPD_{obs} - mean(MPD_{exp})}{std(MPD_{exp})} \quad \text{(Equation 1)}$$

where MPD_{obs} is the observed mean pairwise phylogenetic distance among species in the observed community and MPD_{exp} is calculated from a large sample of randomly drawn communities (Webb, 2000). Positive values of NRI indicate that species in an assemblage (i.e. species that co-occur within a specific community) are more closely related than expected by chance (phylogenetically clustered). Negative values of NRI indicate that species in an assemblage are more distantly related than expected by chance (phylogenetically even). NRI values of zero indicate phylogenetic randomness (Webb, 2000; Webb *et al.*, 2002).

As with body mass dispersion, we compared the outcome of two null models available in the picante R package (Kembel *et al.*, 2014). The first involved shuffling the taxon labels across the species by grid cell occurrence matrix, which maintains the grid cell richness but not species occupancy (equivalent results to shuffling the tips of the phylogenetic tree). The second was the independent swap algorithm, which retains both grid cell richness and species occupancy, a desirable property for ecophylogenetics (Gotelli, 2000; Kembel & Hubbell, 2006; Hardy, 2008; Kembel, 2009). Both null models produced curves of similar shape (Fig. 2B; Fig. S1B). We have therefore chosen only to discuss the latter.

Estimating Rates of Co-occurrence.—

The Checkerboard or C-score quantifies how frequently two species co-occur at a series of sites (Stone & Roberts, 1990). C-scores (varying between zero and one) are highest amongst species with limited or non-existent range overlap and lowest for species pairs whose ranges overlap heavily or otherwise show no apparent disassociation (Stone & Roberts, 1990). Prior to this study, C-scores have been tabulated only amongst pairs of species. Herein, we average the C-scores across all species found in individual assemblages, an approach which to our

knowledge has never before been employed. We average C-scores to identify areas of faunal mixing because average C-scores should, for example, reveal regions of range overlap for species that otherwise do not co-occur. That is, regions of faunal mixing should have the highest average C-scores.

For each pair of species in each grid cell, we calculated checkerboard scores or C-scores. C-scores (C_{ij}) are calculated as:

$$C_{ij} = \frac{(r_i - s_{ij})(r_j - s_{ij})}{(r_i + r_j - s_{ij})} \quad \text{(Equation 2)}$$

where r_i is the number of sites in which species i occurs, r_j is the number of sites in which species j occurs, and S_{ij} is the number at which both species occur (Stone & Roberts, 1990). The term in the denominator standardizes the C-score for differences in the number of sites, in this case grid cells, among occurrence matrices. A large C-score indicates that two species do not co-occur frequently while a low C-score indicates that the distributions of two species show high overlap (Stone & Roberts, 1990). We then averaged the C-scores for species co-occurring in each grid cell to identify areas of faunal mixing.

We used the independent swap algorithm of (Gotelli, 2000) to generate randomized communities and re-calculate average C-scores for each grid cell. As with BM_{dist}, we calculated standardized effect sizes for each grid cell.

Missing Data.—

Because there are several species for which we do not possess body size data, we evaluated whether their exclusion may have introduced systematic biases. We replaced missing body mass data with genus averages and re-calculated BM_{dist}, NRI, and C-scores for all grid cells (1300 species). For BM_{dist} and NRI, we used only the independent swap algorithm to generate null models. We found no major differences and thus performed all analyses using the original

sample of 1070 species (i.e. we did not include species with genus averaged body mass in the final set of analyses or in tests for phylogenetic signal as described above).

Grid cell size.—

To test for the effect of our choice of 100 km by 100 km grid cells, we produced a grid cell by species occurrence matrix with 50 km by 50 km grid cells (although small grid cells are known to be biased) (Hurlbert & Jetz, 2007). We re-calculated BM_{dist}, NRI (using the independent swap algorithm), and average C-scores, as above.

Modelling Body Mass Dispersion.—

We extracted mean annual temperature (MAT) and mean annual precipitation (MAP) data for each grid cell from Climate Wizard (www.climatewizard.org) for the period of 1951-2006 (Girvetz *et al.*, 2009). We did not fit models with Potential Evapotranspiration (PET) because PET is highly co-linear with mean annual temperature.

We partitioned Western Hemispheric mammals among the categories of tropical (-23.4 to 23.4°N), northern temperate (>23.4°N), and southern temperate (< -23.4°N). We used a cut off of 23.4° because it represents the known extent of the tropical belt.

For each region, we modelled average BM_{dist} in each grid cell as a function of NRI, MAP, MAT, C-scores, and species richness using a generalized least squares method with a Gaussian spatial correlation structure, thus accounting for spatial autocorrelation (Moran's I for BM_{dist} = 0.43, $p < 0.001$). We chose to use BM_{dist} as the response variable because, given classical niche theory and the significant phylogenetic signal of mammal body size, body mass dispersion is expected to change in response to changes phylogenetic relatedness and the appearance or disappearance of new species.

We used an information theoretic approach to select the best fit model based on AIC_c (dredge in the MuMIn R package, (Bartoń, 2013)) and partitioned the explained variance in BM_{dist} using adjusted R-squared values (varpart function in the vegan R package; (Oksanen *et al.*, 2012). That is, we selected the best fit model from all possible models (including the null model), which were automatically fit in R, including subsets of the independent variables NRI, MAP, MAT, C-scores, and species richness. We also used model averaging to calculate averaged coefficients and the importance values of model terms, which were calculated as the sum of Akaike weights over all the candidate models with ΔAIC_c of 10 or less relative to the best fit model (Burnham & Anderson, 2002; Bartoń, 2013). An importance of 1.0 indicates that an independent variable is found in all of the candidate models with ΔAIC_c of 10 or less.

Modelling Dispersal Rates.—

We defined the geographic range of each Northern Hemisphere species as, tropical (occurring only within the tropics), southern temperate (occurring only in the southern temperate zone), northern temperate (occurring only in the northern temperate zone), or some combination thereof (occupying two or more of the three regions) (Fig. 1B).

To test for differences in dispersal rates among regions the tropical and temperate zones, we used Biogeographical Stochastic Mapping (BSM) in the BioGeoBears R package (Ree & Smith, 2008) (Matzke, 2013; Matzke, 2014, 2016). BSM uses a maximum likelihood approach to fit a model of Dispersal-Extinction Cladogenesis (DEC) including founder event speciation (DEC + J) (Ree & Smith, 2008). The DEC + J model allows for four types of dispersal events during speciation, i) both species retain the ancestral range, ii) a new species retains only part of the ancestral range, iii) vicariance, and iv) a new species evolves a new range separate from the ancestral range (Matzke, 2013; Matzke, 2014, 2016). Similar models of character evolution, such

as those employed in the phytools R package (Revell, 2011), typically assume no character change at cladogenesis. The DEC + J model differs by allowing for both change along branches (anagenesis) and at nodes (speciation events) (Ree *et al.*, 2005; Ree & Smith, 2008).

Because the DEC + J model requires a fully dichotomous phylogenetic tree, we created a posterior distribution of 100 phylogenetic trees by randomly resolving polytomies (100 iterations required ~15 hours of computation time alone) and calculated dispersal rates for each resolved tree using the DEC + J model employed in the BioGeoBears package.

Results

Western hemisphere mammal body mass shows significant phylogenetic signal ($\lambda = 0.9$; $p < 0.001$; Fig. 1A). Mammals show greatest body mass dispersion (BM_{dist}) in grid cells at high northern latitudes and the lowest in the tropics and some parts of the southern temperate zone (Fig. 2A; Fig. S1A). Tropical mammal body mass dispersion is clustered or random depending on the null model (Fig. 2A, light gray are null assemblages; Fig. S1A). Northern temperate mammals show increasing evenness of body sizes with latitude (Fig. 2A, reduced overlap with null assemblages; Fig. S1A) and have the highest standardized effect sizes (Fig. S2A; Fig. 3A). We have not calculated p-values nor used an arbitrary cut off to judge significance. There are slight differences between the null models (Fig. 2A; Fig. S3A), primarily in terms of whether we find tropical body mass dispersion to be random or under dispersed, but we retain a focus on the null models from the independent swap algorithm due to its desirable statistical properties. There are no apparent pattern differences when BM_{dist} is calculated using genus-averaged body masses (Fig. S4A), herbivores and omnivores alone (Fig. S5A), or finer grid cells (Fig. S6A).

Tropical mammal assemblages show phylogenetic evenness (Fig. 2B; Fig. S1B) regardless of null model choice (Fig. S3B). In the Southern Temperate region, assemblages

become increasingly phylogenetically clustered toward the southern tip of South America (Fig. 2B; Fig. S1B). Northern Temperate mammals show nearly uniform phylogenetic clustering (Fig. 2B; Fig. S1B).

Average C-scores are generally low at tropical latitudes, although the total range is quite large (Fig. 2C; Fig. S1C), reflecting mammal endemicity in the modern tropics. C-scores increase in the northern tropics at the transition zone between the tropics and north temperate regions, indicating a zone of range overlap between tropical and Northern Temperate species (a zone comprised of "bridge species"; Fig. 2C; Fig. S1C). In the northern temperate zone, assemblage-averaged C-scores decline from low latitude to high, reaching values comparable to the tropics at high latitudes, indicating high rates of species range overlap in the Arctic (Fig. 2C; Fig. S1C). In the southern temperate zone, C-scores are highly variable but particularly high in the west (Fig. 2C; Fig. S1C), reflecting faunal mixing in the Mountainous region of the Andes.

Standardized effect sizes for C-score are generally large (and negative; Fig. S2B; Fig. 3C), showing the increased range overlap of otherwise segregated species in null assemblages. The highest SES values (less negative) occur nearest the poles (Fig. S2B; Fig. 3C) where species tend to have larger geographic ranges and thus co-occur most frequently and where the standard deviation of the null assemblage C-scores are highest. The lowest SES values occur in areas of greatest faunal mixing, at the transition zones between the tropics and temperate zones (Fig. S2B; Fig. 3C) and where standard deviations of the null assemblage C-scores are lowest. Although there is a statistically significant decrease in assemblage-averaged C-scores with increasing geographic range size (Fig. S7), the effect size is low ($R^2 = 0.22$). Averaged C-scores for cells at the tropical-temperate transition zones also lie well above the regression line (Fig. S7;

red points). Co-existence of otherwise segregated species in these transition zones is greater than predicted by the relationship between geographic range size and assemblage-averaged C-scores.

All assemblage metrics used here show a high rate of change where the landmass is narrowest (between approximately 10 and 20°N) (Fig. 2A-C; Fig. S1A-C), suggesting that continental narrowing does act as a biodiversity filter. However, the effect is less apparent for BM_{dist} than the other metrics used in this study (Fig. 2A; Fig. S1A).

The full model, which includes mean annual precipitation (MAP), mean annual temperature (MAT), C-scores, species richness, and NRI, was best fit to Northern Temperate mammal BM_{dist} (Table 2; Table S1). Mean annual temperature (MAT) explains the vast amount of model variance (Table 2; Table S1; Fig. 4B).

The best fit model of Southern Temperate mammal BM_{dist}, which includes species richness, MAP, MAT, and NRI, explains very little model variance (Table 2; Table S1), suggesting a limited role for climate filtering and species-species interactions in South America at the scale of our analysis.

The best fit model of tropical mammal BM_{dist} includes average C-scores, NRI, species richness, and MAP (Table 2; Table S1). Average C-scores account for the vast majority of the model variance (Table 2; Table S1), which is probably a result of the commonness of larger-bodied bridge species (i.e., species that bridge the tropical and temperate zones) at the tropical-temperate transition. Although mean annual precipitation is a significant correlate of BM_{dist} in tropical mammals, it explains a relatively small amount of model variance (Table 2; Fig. 4A).

Overall, dispersal both into and out of the tropics is highest, suggesting that the tropics have acted as both a biodiversity pump and a sink. Direct exchanges between the temperate zones are comparatively rare because dispersal events between them necessarily involves an

intermediate stage range expansion across the tropics (i.e. species that occupy both tropical and temperate zones which are known as bridge species; Table 3). Dispersals from the tropics into the northern temperate zone are also comparatively rare, possibly reflecting the narrow land connection between them (Table 3). Dispersal between the tropical zone and southern temperature zone is most common (Table 3).

Discussion

Differences in the primary drivers of community assembly have been proposed to explain disparate richness and community structure among the tropical and temperate regions of the world. Using body size dispersion and phylogenetic diversity, we show that in the Western Hemisphere, i) tropical mammal body masses are clustered, despite apparent phylogenetic evenness, providing no support for environmental filtering, character displacement nor competitive exclusion as important community assembly mechanisms at the grain of our analysis, ii) the high body mass dispersion and phylogenetic clustering of Northern Temperate mammals supports the operation of both a climate filtering and competitively-driven character displacement, and iii) Southern Temperate mammal body mass dispersion is not distinguishable from random, suggesting a limited role of climate filtering and species-species interactions at the grain of our analysis. We find that the tropical-temperate transition zones are characterized by the highest rates of faunal mixing. We also find comparatively high rates of historical dispersal into and out of the tropics, particularly southward, which is expected given the southward-bias of mammal dispersals during the Great American Biotic Interchange (~ 3 Ma; Woodburne, 2010) and episodic dispersals that occurred as early as 20 Ma (Bacon *et al.*, 2015). We therefore suggest an important role of dispersal and faunal mixing in Western Hemisphere mammal community assembly, particularly in the tropical and Southern Temperate zones.

The Northern Temperate Zone is characterized by relatively steep climate gradients (Fig. S8), which might impart strong environmental filters on mammal communities. Classical niche theory predicts that environmental filtering limits the range of traits expressed by co-existing species through exclusion of species with unsuitable niche characteristics (Hawkins *et al.*, 2003; Soininen *et al.*, 2007a; Soininen, 2010). Under an environmental filtering model, we expect progressively declining body mass dispersion (BM_{dist}) and increasing phylogenetic relatedness among species in the same assemblage (higher Net Relatedness Index or NRI) that is correlated with mean annual temperature and precipitation (MAT and MAP; Table 1) (Hawkins *et al.*, 2003; Currie *et al.*, 2004; Helmus *et al.*, 2007; Peres-Neto *et al.*, 2012). However, BM_{dist} diverges from null communities in the Northern Temperate Zone but in the opposite direction as predicted; change in BM_{dist} is correlated with MAT but increases rather than decreases at high latitudes. Two non-mutually exclusive hypotheses might explain increasing dispersion of body size at high northern latitudes: i) a flattening of the body mass distribution (McNab, 1971; Blackburn *et al.*, 1999; Ashton *et al.*, 2000; Freckleton *et al.*, 2003) and ii) character displacement (*in situ* body size evolution) as a result of resource competition (Safi *et al.*, 2011; Oliveira et al. 2016) (Table 1).

High latitude mammal communities typically show flatter body size distributions than their low latitude counterparts (Lyons & Smith, 2013). A flat body size distribution is characterized by similarity in species richness amongst body size categories (typically $\log_{10}$body mass categories) (Brown & Nicoletto, 1991) and may result from either competitive exclusion (via limiting similarity) or character displacement.

High latitude environments, such as those found in the Canadian Arctic, are relatively unproductive environments that limit nutrient availability to individuals, thus presenting both

increasing intensity of resource competition and strong environmental filters (Hawkins *et al.*, 2003; Soininen *et al.*, 2007a; Soininen, 2010). We suggest that flattening of the body size distribution explains our observation of high BM_{dist} and that high latitude, northern hemispheric mammals experience resource competition at the large spatial grain we use herein (also noted by Safi *et al.*, 2011). Furthermore, because we simultaneously observe phylogenetic clustering amongst Northern Hemisphere mammals (that is well explained by MAT), we also suggest that they are subject to environmental filtering (Table 1). Thus, the nutrient limiting, comparatively harsh conditions of the Canadian north (with its short growing season and desert conditions) have limited the types of species present and driven them apart in niche space.

The latitudinal gradient in body mass dispersion that is so apparent in the Northern Temperate zone is much less pronounced in the Southern Temperate region, likely due, in part, to shallower climate gradients (Fig. S8). We therefore find little support for environmental filtering and resource competition as drivers of Southern Temperate mammal community assembly at the grain of our analysis. Overall the dispersion of Southern Temperate mammal body masses bears a strong similarity to tropical assemblages. Historical extinction of large portions of the South American endemic faunas (e.g., Notoungulates) and invasion by placental mammals during the Plio-Pleistocene (Patterson & Pascual, 1968; Webb, 1978; Woodburne, 2010) likely explain the similarity in community structure between southern and tropical mammal faunas.

The remarkable richness of tropical mammal communities might suggest major differences in community assembly mechanisms relative to the comparatively depauperate temperate zones. Traditionally, tropical mammal richness is attributed to finer partitioning of niches (the outcome of heightened resource competition) or enhanced resource availability. At

the grain of our analysis, tropical communities are characterized by a combination of body size clustering (i.e., low BM_{dist}), consistent with other recent studies of functional diversity (Oliveira *et al.*, 2016), and phylogenetic evenness (i.e., low NRI). As such, we find no clear support for a finer niche partitioning nor environmental filtering (given the low explanatory power of the climate variables MAT and MAP) at the grain of our analysis. Note that we do not use a lack of support for species-species interactions at the scale of 100km by 100 km grid cells as definitive evidence that tropical mammals do not experience resource competition. We conclude, however, that resource competition amongst tropical mammals is not apparent at the coarse grain of our analyses. We do, however, suggest that low tropical mammal BM_{dist} results from a peaked body mass distribution; small and medium species dominate tropical faunas (Lyons & Smith, 2013), reflecting enhanced energy and resource availability (Currie, 1991; Oliveira *et al*., 2016) rather than resource competition.

If we find no support for species-species interactions nor climate filtering as the primary drivers of community assembly, what then accounts for tropical phylogenetic evenness and high level of similarity in BM_{dist} between the tropical and Southern temperate zones at the scale of our analysis? Enhanced resource availability does not necessarily predict phylogenetic evenness. However, long-distance dispersals of species from the tropics outward (e.g. a tropical diversity pump; particularly southward thus increasing faunal similarity) and from the temperate zones into the tropics (e.g. a tropical diversity sink) (Leighton, 2005; Jablonski *et al.*, 2006; Rolland *et al.*, 2015) may explain tropical phylogenetic evenness.

There have been a number of dispersal events among the tropical and temperate zones in the Western Hemisphere (Table 3). Historical mammalian dispersals between the Northern Temperate and tropical zones are, however, comparatively rare (Table 3), reflecting the relative

isolation of the North American and South American continents and limited exchange of species prior to the Oligocene-Miocene transition and the Pliocene when the Isthmus of Panama was definitively closed (~3 Ma) (Woodburne, 2010; Bacon *et al.*, 2015). Similarly, direct exchanges of species between temperate zones are rare (Table 3), largely because the tropics must act as an intermediary or land bridge, a role that is apparent in the high assemblage-averaged C-scores at the tropical-temperate transition zones (Fig. 2C). As predicted, however, rates of historical dispersal from the northern to southern temperate zone are higher than the reverse, reflecting the higher frequency of southward than northward dispersals particularly during the Great American Biotic Interchange (Woodburne, 2010) but also as early as 20 Ma (Miocene; Bacon et al. 2015).

Overall, rates of dispersal into and out of the tropics are highest (Table 3), suggesting that tropical mammal community structure may be a product of dispersal events and faunal mixing among biogeographic regions. Together, a tropical biodiversity pump and immigration of new, more distantly related species into the tropics may have contributed to the apparent phylogenetic evenness of mammal communities there. The highest of all transition rates occurs between the tropics and Southern Temperate zone (Table 3), suggesting that the land connection between the two has been important in facilitating species exchange and faunal mixing. Decreased isolation and increasing faunal mixing of tropical and Southern Temperate faunas might explain their relative similarity in BM_{dist} and the limited power of climate to explain South American mammal community structure.

Recent studies suggest that knowledge of the past is required to understand the assembly of modern communities (Cardillo, 2011; Fraser *et al.*, 2014; Fraser *et al.*, 2015; Maguire *et al.*, 2015; Rowan *et al.*, 2016) and that patterns of extinction and speciation alone can lead to changes in phylogenetic community structure (Fraser *et al.*, 2015). Inclusion of extinct species in

these types of analyses would likely illuminate the contribution of differences in historical rates of speciation and extinction, which cannot be accurately estimated from extant-only phylogenies, to differences in community structure among the tropical and temperate zones. We have shown that the model of competition *vs*. environmental filtering, which is pervasive in the macroecological literature, is oversimplified. Community assembly is a complex process dependent on both historical (e.g. dispersal and speciation/extinction) as well as contemporary (e.g. climate filtering, competition for resources) drivers.

Acknowledgements

We thank all of the contributors to the NatureServe Canada, PanTHERIA, Elton traits 1.0, and Climate Wizard databases that provided the bulk of the data for this paper. We thank Jonathan Davies for serving as editor of this paper. We also thank Fabien Condamine and four anonymous reviewers for helpful reviews of a previous iteration of this manuscript. We also thank Dr. Peter Buck and the Smithsonian Institution for a Peter Buck Postdoctoral Fellowship awarded to D. Fraser. We thank J. Ludtke and E. Lightner for providing comments on an earlier version of this manuscript. We also thank members of the Evolution of Terrestrial Ecosystems working group as well as A. Du and A. Jukar for discussion regarding this paper. This paper was supported, in part, by NSF-DEB 1257825. This is ETE publication number 343.

Literature Cited

Ashton, K.G., Tracy, M.C. & Queiroz, A.d. (2000) Is Bergmann's rule valid for mammals? *American Naturalist*, **156**, 390-415.

Bacon, C.D., Silvestro, D., Jaramillo, C., Smith, B.T., Chakrabarty, P. & Antonelli, A. (2015) Biological evidence supports an early and complex emergence of the Isthmus of Panama. *Proceedings of the National Academy of Sciences*, **112**, 6110-6115.

Bartoń, K. (2013) Model selection and model averaging based on information criteria (AICc and alike).

Baselga, A., Lobo, J.M., Svenning, J.-C., Aragón, P. & Araújo, M.B. (2012) Dispersal ability modulates the strength of the latitudinal richness gradient in European beetles. *Global Ecology and Biogeography*, **21**, 1106-1113.

Belmaker, J. & Jetz, W. (2015) Relative roles of ecological and energetic constraints, diversification rates and region history on global species richness gradients. *Ecology Letters*, **18**, 563-571.

Blackburn, T.M., Gaston, K.J. & Loder, N. (1999) Geographic gradients in body size: a clarification of Bergmann's rule. *Diversity & Distributions*, **5**, 165-174.

Brown, J.H. (1984) On the Relationship between Abundance and Distribution of Species. *The American Naturalist*, **124**, 255-279.

Brown, J.H. & Nicoletto, P.F. (1991) Spatial Scaling of Species Composition: Body Masses of North American Land Mammals. *The American Naturalist*, **138**, 1478-1512.

Buckley, L.B., Davies, J., Ackerly, D.D., Kraft, N.J.B., Harrison, S.P., Anacker, B.L., Cornell, H.V., Damschen, E.I., Grytnes, J.-A., Hawkins, B.A., McCain, C.M., Stephens, P.R. & Wiens, a.J.J. (2010) Phylogeny, niche conservatism and the latitudinal diversity gradient in mammals. *Proceedings of the Royal Society, Series B*, **277**, 2121-2138.

Burnham, K.P. & Anderson, D.R. (2002) *Model selection and multimodel inference: a practical information-theoretic approach, 2nd ed.* Springer, New York, New York.

Cadotte, M., Albert, C.H. & Walker, S.C. (2013) The ecology of differences: assessing community assembly with trait and evolutionary distances. *Ecology Letters*, **16**, 1234-1244.

Cantalapiedra, J.L., Fernández, M.H. & Morales, J. (2014) The biogeographic history of ruminant faunas determines the phylogenetic structure of their assemblages at different scales. *Ecography*, **37**, 1-9.

Cardillo, M. (2011) Phylogenetic structure of mammal assemblages at large geographical scales: linking phylogenetic community ecology with macroecology. *Philosophical Transactions of the Royal Society B*, **366**, 2545-2553.

Cavender-Bares, J., Keen, A. & Miles, B. (2006) Phylogenetic Structure of Floridian Plant Communities Depends on Taxonomic and Spatial Scale. *Ecology*, **87**, S109-S122.

Cavender-Bares, J., Kozak, K.H., Fine, P.V.A. & Kembel, S.W. (2009) The merging of community ecology and phylogenetic biology. *Ecology Letters*, **12**, 693-715.

Condamine, F.L., Sperling, F.A.H., Wahlberg, N., Rasplus, J.-Y. & Kergoat, G.J. (2012) What causes latitudinal gradients in species diversity? Evolutionary processes and ecological constraints on swallowtail biodiversity. *Ecology Letters*, **15**, 267-277.

Connor, E.F. & Simberloff, D. (1979) The assembly of species communities: chance or competition? *Ecology*, **60**, 1132-1140.

Currie, D.J. (1991) Energy and large-scale patterns of animal- and plant-species richness. *The American Naturalist*, **137**, 27-49.

Currie, D.J., Mittelbach, G.G., Cornell, H.V., Field, R., Guegan, J.-F., Hawkins, B.A., Kaufman, D.M., Kerr, J.T., Oberdorff, T., O'Brien, E. & Turner, J.R.G. (2004) Predictions and tests of climate-based hypotheses of broad-scale variation in taxonomic richness. *Ecology Letters*, **7**, 1121–1134.

Damuth, J. (1981) Population Density and body size in mammals. *Nature*, **290**, 699-700.

Dobrovolski, R., Melo, A.S., Cassemiro, F.A.S. & Diniz-Filho, J.A.F. (2012) Climatic history and dispersal ability explain the relative importance of turnover and nestedness components of beta diversity. *Global Ecology and Biogeography*, **21**, 191-197.

Faurby, S. & Svenning, J.-C. (2015) Historic and prehistoric human-driven extinctions have reshaped global mammal diversity patterns. *Diversity and Distributions*, 1-12.

Fine, P. & Ree, R. (2006) Evidence for a Time Integrated Species Area Effect on the latitudinal gradient in tree diversity. *The American Naturalist*, **168**, 796-804.

Fine, P.V.A. (2015) Ecological and Evolutionary Drivers of Geographic Variation in Species Diversity. *Annual Review of Ecology, Evolution, and Systematics*, **46**, 369-392.

Fraser, D., Gorelick, R. & Rybczynski, N. (2015) Macroevolution and climate change influence phylogenetic community assembly of North American hoofed mammals. *Biological Journal of the Linnean Society*, **114**, 485-494.

Fraser, D., Hassall, C., Gorelick, R. & Rybczynski, N. (2014) Mean annual precipitation explains spatiotemporal patterns of Cenozoic mammal beta diversity and latitudinal diversity gradients in North America. *PloS One*, **9**, e106499.

Freckleton, R.P., Harvey, P.H. & Pagel, M. (2003) Bergmann's rule and body size in mammals. *The American Naturalist*, **161**, 821-825.

Fritz, S.A. & Purvis, A. (2010) Phylogenetic diversity does not capture body size variation at risk in the world's mammals. *Proceedings of the Royal Society of London B: Biological Sciences*, **277**, 2435-2441.

Fritz, S.A., Bininda-Emonds, O.R.P. & Purvis, A. (2009) Geographical variation in predictors of mammalian extinction risk: big is bad, but only in the tropics. *Ecology Letters*, **12**, 538-549.

Girvetz, E.H., Zganjar, C., Raber, G.T., Maurer, E.P., Kareiva, P. & Lawler, J.J. (2009) Applied climate-change analysis: the climate wizard tool. *PLoS One*, **4**, e8320.

Gotelli, N.J. (2000) Null model analysis of species co-occurrence patterns. *Ecology*, **81**, 2606-2621.

Gotelli, N.J. & Entsminger, G.L. (2001) Swap and fill algorithms in null model analysis: rethinking the knight's tour. *Oecologia*, **129**, 281-291.

Green, W.A., Hunt, G., Wing, S.L. & DiMichele, W.A. (2011) Does extinction wield an axe or pruning shears? How interactions between phylogeny and ecology affect patterns of extinction. *Paleobiology*, **37**, 72-91.

Hardy, O.J. (2008) Testing the spatial phylogenetic structure of local communities: statistical performances of different null models and test statistics on a locally neutral community. *Journal of Ecology*, **96**, 914-926.

Hawkins, B.A., Field, R., Cornell, H.V., Currie, D.J., Guegan, J.-F., Kaufman, D.M., Kerr, J.T., Mittelbach, G.G., Oberdorff, T., O'Brien, E.M., Porter, E.E. & Turner, J.R.G. (2003) Energy, water, and broad-scale geographic patterns of species richness. *Ecology*, **84**, 3105-3117.

Helmus, M.R., Savage, K., Diebel, M.W., Maxted, J.T. & Ives, A.R. (2007) Separating the determinants of phylogenetic community structure. *Ecology Letters*, **10**, 917-925.

Hunt, G. (2013) Testing the link between phenotypic evolution and speciation: an integrated palaeontological and phylogenetic analysis. *Methods in Ecology and Evolution*, **4**, 714-723.

Hurlbert, A.H. & Jetz, W. (2007) Species richness, hotspots, and the scale dependence of range maps in ecology and conservation. *Proceedings of the national academy of sciences*, **104**, 13384-13389.

Jablonski, D. (1993) The tropics as a source of evolutionary novelty through geological time. *Nature*, **364**, 142-144.

Jablonski, D., Roy, K. & Valentine, J.W. (2006) Out of the tropics: evolutionary dynamics of the latitudinal diversity gradient. *Science*, **314**, 102-106.

Jablonski, D., Belanger, C.L., Berke, S.K., Huang, S., Krug, A.Z., Roy, K., Tomasovych, A. & Valentine, J.W. (2013) Out of the tropics, but how? Fossils, bridge species, and thermal ranges in the dynamics of the marine latitudinal diversity gradient. *Proceedings of the National Academy of Sciences USA*, **110**, 10487-10494.

Jetz, W. & Fine, P.V.A. (2012) Global Gradients in Vertebrate Diversity Predicted by Historical Area-Productivity Dynamics and Contemporary Environment. *PLoS Biology*, **10**, e1001292.

Jocque, M., Field, R., Brendonck, L. & Meester, L.D. (2010) Climatic control of dispersal–ecological specialization trade-offs: a metacommunity process at the heart of the latitudinal diversity gradient? *Global Ecology and Biogeography*, **19**, 244-252.

Johnson, C.N. (2002) Determinants of loss of mammal species during the Late Quaternary 'megafauna' extinctions: life history and ecology, but not body size. *Proceedings of the Royal Society of London B*, **269**, 2221-2227.

Jones, K.E., Bielby, J., Cardillo, M., Fritz, S.A., O'Dell, J., Orme, C.D.L., Safi, K., Sechrest, W., Boakes, E.H., Carbone, C., Connolly, C., Cutts, M.J., Foster, J.K., Grenyer, R., Habib, M., Plaster, C.A., Price, S.A., Rigby, E.A., Rist, J., Teacher, A., Bininda-Emonds,

O.R.P., Gittleman, J.L., Mace, G.M. & Purvis, A. (2009) PanTHERIA: a species-level database of life history, ecology, and geography of extant and recently extinct mammals. *Ecology*, **90**, 2648.

Kembel, S.W. (2009) Disentangling niche and neutral influences on community assembly: assessing the performance of community phylogenetic structure tests. *Ecology Letters*, **12**, 949-960.

Kembel, S.W. & Hubbell, S.P. (2006) The phylogenetic structure of a neotropical forest tree community. *Ecology*, **87**, S86-S99.

Kembel, S.W., Ackerly, D.D., Blomberg, S., Cornwell, W.K., Cowan, P.D., Helmus, M.R., Morlon, H. & Webb, C.O. (2014) R tools for integrating phylogenies and ecology. https://cran.r-project.org/web/packages/picante/index.html.

Kraft, N.J.B., Cornwell, W.K., Webb, C.O. & Ackerly, D.D. (2007) Trait evolution, community assembly, and phylogenetic structure of ecological communities. *The American Naturalist*, **170**, 271-283.

Lamanna, C., Blonder, B., Violle, C., Kraft, N.J.B., Sandel, B., Šímová, I., II, J.C.D., Svenning, J.-C., McGill, B.J., Boyle, B., Buzzard, V., Dolins, S., Jørgensen, P.M., Marcuse-Kubitza, A., Morueta-Holme, N., Peet, R.K., Piel, W.H., Regetz, J., Schildhauer, M., Spencer, N., Thiers, B., Wiser, S.K. & Enquist, B.J. (2014) Functional trait space and the latitudinal diversity gradient. *Proceedings of the National Academy of Sciences USA*, **111**, 13745-13750.

Leighton, L.R. (2005) The latitudinal diversity gradient through deep time: testing the ‘‘Age of the Tropics’’ hypothesis using Carboniferous productidine brachiopods. *Evolutionary Ecology*, **19**, 563-581.

Lyons, S.K. & Willig, M.R. (1999) A hemispheric assessment of scale dependence in latitudinal gradients of species richness. *Ecology*, **80**, 2483-2491.

Lyons, S.K. & Willig, M.R. (2002) Species richness, latitude, and scale-sensitivity. *Ecology*, **83**, 47-58.

Lyons, S.K. & Smith, F.A. (2013) Macroecological patterns of body size in mammals across time and space. *Animal body size: linking patterns and process across space, time and taxonomy* (ed. by F.A. Smith and S.K. Lyons), pp. 116-144. University of Chicago Press, Chicago.

Lyons, S.K., Amatangelo, K.L., Behrensmeyer, A.K., Bercovici, A., Blois, J.L., Davis, M., DiMichele, W.A., Du, A., Eronen, J.T., Tyler Faith, J., Graves, G.R., Jud, N., Labandeira, C., Looy, C.V., McGill, B., Miller, J.H., Patterson, D., Pineda-Munoz, S., Potts, R., Riddle, B., Terry, R., TÃ³th, A., Ulrich, W., VillaseÃ±or, A., Wing, S., Anderson, H., Anderson, J., Waller, D. & Gotelli, N.J. (2016) Holocene shifts in the assembly of plant and animal communities implicate human impacts. *Nature*, **529**, 80-83.

MacArthur, R. & Levins, R. (1967) The limiting similarity, convergence and divergence of coexisting species. *The American Naturalist*, **101**, 377-385.

Maguire, K.C., Nieto-Lugilde, D., Fitzpatrick, M.C., Williams, J.W. & Blois, J.L. (2015) Modeling species and community responses to past, present, and future episodes of climatic and ecological Change. *Annual Review of Ecology, Evolution, and Systematics*, **46**, 343-368.

Mannion, P.D., Upchurch, P., Benson, R.B.J. & Goswami, A. (2014) The latitudinal biodiversity gradient through deep time. *Trends in Ecology and Evolution*, **29**, 42-50.

Marcot, J.D., Fox, D.L. & Niebuhr, S.R. (2016) Late Cenozoic onset of the latitudinal diversity gradient of North American mammals. *Proceedings of the National Academy of Sciences*, **113**, 7189-7194.

Martin, R.A. & Pfennig, D.W. (2009) Disruptive selection in natural populations: the roles of ecological specialization and resource competition. *The American Naturalist*, **174**, 268-281.

Matzke, N.J. (2013) Probabilistic historical biogeography: new models for founder-event speciation, imperfect detection, and fossils allow improved accuracy and model-testing. *Frontiers in Biogeography*, **5**, 242-248.

Matzke, N.J. (2014) Model Selection in Historical Biogeography Reveals that Founder-event Speciation is a Crucial Process in Island Clades. *Systematic Biology*, **63**, 951-970.

Matzke, N.J. (2016) *Stochastic mapping under biogeographical models*. PhyloWiki BioGeoBEARS website, 2016, http://phylo.wikidot.com/biogeobears#stochastic_mapping

Mayfield, M.M. & Levine, J.M. (2010) Opposing effects of competitive exclusion on the phylogenetic structure of communities. *Ecology Letters*, **13**, 1085-1093.

Mazel, F., Wüest, R.O., Gueguen, M., Renaud, J., Ficetola, G.F., Lavergne, S. & Thuiller, W. (2017) The geography of ecological niche evolution in mammals. *Current Biology*, **27**, 1369-1374.

McNab, B.K. (1971) On the ecological significance of Bergmann's rule. *Ecology*, **52**, 845-854.

McPeek, M.A. (2008) The ecological dynamics of clade diversification and community assembly. *The American Naturalist*, **172**, E270-E284.

Mittelbach, G.G., Schemske, D.W., Cornell, H.V., Allen, A.P., Brown, J.M., Bush, M.B., Harrison, S.P., Hurlbert, A.H., Knowlton, N., Lessios, H.A., McCain, C.M., McCune, A.R., McDade, L.A., McPeek, M.A., Near, T.J., Price, T.D., Ricklefs, R.E., Roy, K., Sax, D.F., Schluter, D., Sobel, J.M. & Turelli, M. (2007) Evolution and the latitudinal diversity gradient: speciation, extinction and biogeography. *Ecology Letters*, **10**, 315-331.

Morales-Castilla, I., Olalla-Tárraga, M.Á., Purvis, A., Hawkins, B.A. & Rodríguez, M.Á. (2012) The Imprint of Cenozoic migrations and evolutionary history on the biogeographic gradient of body size in New World mammals. *The American Naturalist*, **180**, 246-256.

Oksanen, J., Blanchet, F.G., Roeland Kindt, P.L., Minchin, P.R., O'Hara, R.B., Simpson, G.L., Solymos, P., Stevens, M.H.H. & Wagner, H. (2012) *Package vegan version 2.0-7*.

Oliveira, B.F., Machac, A., Costa, G.C., Brooks, T.M., Davidson, A.D., Rondinini, C. & Graham, C.H. (2016) Species and functional diversity accumulate differently in mammals. *Global Ecology and Biogeography*, **25**, 1119–1130.

Patterson, B. & Pascual, R. (1968) The fossil mammal fauna of South America. *The Quarterly Review of Biology*, **43**, 409-451.

Patterson, B.D., Ceballos, G., Sechrest, W., Tognelli, M.F., Brooks, T., Luna, L., Ortega, P., Salazar, I. & Young, B.E. (2007) Digital distribution maps of the mammals of the Western Hemisphere, version 3.0. NatureServe, Arlington, Virginia, USA.

Peres-Neto, P.R., Leibold, M.A. & Dray, S. (2012) Assessing the effects of spatial contingency and environmental filtering on metacommunity phylogenetics. *Ecology*, **93**, S14-S30.

Peters, R.H. (1983) The ecological implications of body size. Cambridge University Press, New York.

Pineda-Munoz, S., Evans, A.R. & Alroy, J. (2016) The relationship between diet and body mass in terrestrial mammals. *Paleobiology*, **42**, 659-669.

Polly, P.D., Fuentes-Gonzalez, J., Lawing, A.M., Bormet, A.K. & Dundas, R.G. (2017) Clade sorting has a greater effect than local adaptation on ecometric patterns in Carnivora. *Evolutionary Ecology Research*, **18**, 61-95.

Qian, H., Zhang, Y., Zhang, J. & Wang, X. (2013) Latitudinal gradients in phylogenetic relatedness of angiosperm trees in North America. *Global Ecology and Biogeography*, **22**, 1183-1191.

Razafindratsima, O.H., Mehtani, S. & Dunham, A.E. (2012) Extinctions, traits and phylogenetic community structure: insights from primate assemblages in Madagascar. *Ecography*, **35**, 1-10.

Ree, R.H. & Smith, S.A. (2008) Maximum likelihood inference of geographic range evolution by dispersal, local extinction, and cladogenesis. *Systematic Biology*, **57**, 4-14.

Ree, R.H., Moore, B.R., Webb, C.O. & Donoghue, M.J. (2005) A likelihood framework for inferring the evolution of geographic range on phylogenetic trees. *Evolution*, **59**, 2299-2311.

Revell, L.J. (2011) phytools: an R package for phylogenetic comparative biology (and other things). *Methods in Ecology and Evolution*, **3**, 217-223.

Revell, L.J. (2013) Two new graphical methods for mapping trait evolution on phylogenies. *Methods in Ecology and Evolution*, **4**, 754-759.

Ricklefs, R.E. 1987. Community diversity: relative roles of local and regional processes. *Science*, **235**, 167-171.

Ricklefs, R.E. (2010) Evolutionary diversification, coevolution between populations and their antagonists, and the filling of niche space. *Proceedings of the National Academy of Sciences USA*, 1-8.

Rolland, J., Condamine, F.L., Jiguet, F. & Morlon, H.l. (2014) Faster speciation and reduced extinction in the tropics contribute to the mammalian latitudinal diversity gradient. *PLoS One*, **12**, e1001775.

Rolland, J., Condamine, F.L., Beeravolu, C.R., Jiguet, F. & Morlon, H. (2015) Dispersal is a major driver of the latitudinal diversity gradient of Carnivora. *Global Ecology and Biogeography*, **24**, 1059-1071.

Rose, P.J., Fox, D.L., Marcot, J. & Badgley, C. (2011) Flat latitudinal gradient in Paleocene mammal richness suggests decoupling of climate and biodiversity. *Geology*, **39**, 163-166

Rosenzweig, M.L. (1995) *Species diversity in space and time*. Cambridge University Press, Cambridge.

Rowan, J., Kamilar, J.M., Beaudrot, L. & Reed, K.E. (2016) Strong influence of palaeoclimate on the structure of modern African mammal communities. *Proceedings of the Royal Society B: Biological Sciences*, **283,** 20161207.

Safi, K., Cianciaruso, M.V., Loyola, R.D., Brito, D., Armour-Marshall, K. & Diniz-Filho, J.A.F. (2011) Understanding global patterns of mammalian functional and phylogenetic diversity. *Philosophical Transactions of the Royal Society B*, **366**, 2536-2544.

Schoener, T.W. (1974) Resource Partitioning in Ecological Communities. *Science* **185**, 27-39.

Smith, F.A., Brown, J.H., Haskell, J.P., Lyons, S.K., Alroy, J., Charnov, E.L., Dayan, T., Enquist, B.J., Morgan Ernest, S.K., Hadly, E.A., Jones, K.E., Kaufman, D. M., Marquet, P.A., Maurer, B.A., Niklas, K.J., Porter, W.P., Tiffney, B., & Willig, M.R. (2004)

Similarity of Mammalian Body Size across the Taxonomic Hierarchy and across Space and Time. *The American Naturalist*, **163**, 672-691.

Soininen, J. (2010) Species turnover along abiotic and biotic gradients: patterns in space equal patterns in time? *BioScience*, **60**, 433-439.

Soininen, J., Lennon, J.J. & Hillebrad, H. (2007a) A multivariate analysis of beta diversity across organisms and environments. *Ecology*, **88**, 2830-2838.

Soininen, J., McDonald, R. & Hillebrand, H. (2007b) The distance decay of similarity in ecological communities. *Ecography*, **30**, 3-12.

Stone, L. & Roberts, A. (1990) The checkerboard score and species distributions. *Oecologia*, **85**, 74-79.

Vermeij, G.J. (2005) Invasion as expectation. *Species invasions: insight into ecology, evolution and biogeography* (ed. by D.F. Sax, J.J. Stachowicz and S.D. Gaines), pp. 315-339. Sinauer Associates, Sunderland, MA.

Webb, C.O. (2000) Exploring the phylogenetic structure of ecological communities: an example for rain forest trees. *American Naturalist*, **156**, 145-155.

Webb, C.O., Ackerly, D.D., McPeek, M.A. & Donoghue, M.J. (2002) Phylogenies and community ecology. *Annual Review of Ecology and Systematics*, **33**, 475-505.

Webb, S.D. (1978) A History of Savanna Vertebrates in the New World. Part II: South America and the Great Interchange. *Annual Review of Ecology and Systematics*, **9**, 393-426.

Weir, J.T. (2014) Environmental harshness, latitude, and incipient speciation. *Molecular Ecology*, **23**, 251-253.

Weir, J.T. & Schluter, D. (2007) The latitudinal gradient in recent speciation and extinction rates of birds and mammals. *Science*, **315**, 1574-1576.

Wiens, J.J. & Graham, C.H. (2005) Niche conservatism: integration evolution, ecology, and conservation biology. *Annual Review in Ecology, Evolution, and Systematics*, **36**, 519-539.

Willig, M.R. & Lyons, S.K. (1998) An analytical model of latitudinal gradients of species richness with an empirical test for marsupials and bats in the New World. *Oikos*, **81**, 93-98.

Willig, M.R., Kaufman, D.M. & Stevens, R.D. (2003) Latitudinal gradients of biodiversity: Pattern, Process, Scale, and Synthesis. *Annu. Rev. Ecol. Evol. Syst.* , **34**, 273–309.

Woodburne, M.O. (2010) The Great American Biotic Interchange: dispersals, tectonics, climate, sea level and holding pens. *Journal of Mammalian Evolution*, **17**, 245-264.

Biosketches

Danielle Fraser is interested in the effects of long-term climate changes, biotic interchange, and extinction on the community assembly of fossil and modern vertebrates as well as the factors that have led to the emergence of modern communities.

S. Kathleen Lyons is interested in factors that affect and control species diversity at multiple scales across space and time including the deep time origins of modern ecological patterns and processes.

Tables

Table 1. Summary of predicted models of best fit for each hypothesis. BM_{dist} refers to the average body size disparity between species in a community. NRI is the Net Relatedness Index. All predictions assume niche conservatism. MAP is mean annual precipitation and MAT is mean annual temperature.

Hypothesis	Predicted best fit models	Predicted values of BMdist	Explanation	Predicted relationship
Null	BMdist ~ Intercept	-	-	BMdist is not distinguishable from a random communities with the same species richness.
Environmental filtering	BMdist ~ MAP + Mean Annual Temperature + NRI	BMdist declines from the tropics to the poles; High latitude BMdist shows clustering	Classical niche theory predicts the climate filtering leads to trait clustering; it is traditionally assumed that high latitude climates impart a stronger filter	↓ BMdist ~ ↓ MAT; ↓ BMdist ~ ↓ MAP; ↓ BMdist ~ ↑ NRI
Competitive exclusion (via limiting similarity)	BMdist ~ NRI + SR	BMdist declines from the tropics to the poles; Low latitude BMdist shows evenness	Classical niche theory predicts the competition for resources may lead to competitive exclusion; it is traditionally assumed that low latitude faunas are more interactive	↑ BMdist ~ ↓ NRI; ↑ BMdist ~ ↑ SR
Competitive exclusion (via differences in competitive ability)	BMdist ~ NRI + SR	BMdist declines from the tropics to the poles; Low latitude BMdist shows evenness	Coexistence theory predicts the differences in competitive ability may lead to competitive exclusion; it is traditionally assumed that low latitude faunas are more interactive	↓ BMdist ~ ↑ NRI; ↓ BMdist ~ ↑ SR
Character displacement	BMdist ~ NRI + SR	BMdist declines from the tropics to the poles; Low latitude BMdist shows evenness	Classical niche theory predicts the competition for resources may lead to limiting similarity; it is traditionally assumed that low latitude faunas are more interactive	↑ BMdist ~ ↑ NRI; ↑ BMdist ~ ↑ SR

Faunal Mixing	Not modelled using gls	NRI is lowest in the regions in which historical faunal mixing is most frequent; the tropics may have acted as both as source and sink for biodiversity over evolutionary time	Mixing of species with divergent evolutionary histories (i.e., representing a deeper split in the phylogeny) occurs in regions through which biotic interchange occurs	↓ NRI in the Tropics
	Not modelled using gls	Assemblage averaged C-scores are highest in regions with bridge species; the subtropics are where the ranges of tropical and temperate species overlap	Mixing of species that otherwise do not co-occur leads to higher assemblage averaged C-scores	↑ C-scores in the Subtropics

Table 2. Results of best fit models of spatial change in average mammal BMdist in the tropical and temperate regions of the Western Hemisphere. We used generalized least squares models with a Gaussian spatial correlation structure. Model fit was evaluated using AICc. Importances and model averaged coefficients were calculated from models within 10 ΔAICc of the best fit model. NRI is the Net Relatedness Index.

Region	Best fit model	Variance explained (%)	Importance	Model averaged coefficients	t-value	p-value	Supported Hypothesis
Tropics	**Average C-score**	**28.18**	**1.00**	**1.60**	13.07	< 0.001	**Faunal mixing**
	Mean annual precipitation	10.80	0.86	-2.30E-05	-2.33	0.020	
	NRI	6.51	1.00	-0.25	-4.01	< 0.001	
	Species richness	0.14	1.00	-2.83E-03	-6.05	< 0.001	
Northern Temperate	**Mean annual temperature**	**37.62**	**1.00**	**-0.02**	-11.62	< 0.001	**Environmental Filtering/ Character Displacement**
	Mean annual precipitation	19.72	1.00	-2.59E-04	-6.07	< 0.001	
	Average C-score	16.32	1.00	0.75	4.15	< 0.001	
	Species richness	10.97	0.98	-4.77E-03	-3.18	0.001	
	NRI	0.48	1.00	-1.00	-4.73	< 0.001	
Southern Temperate	**Species richness**	**3.11**	**0.80**	-4.79E-03	-2.37	0.018	**Faunal mixing**
	Mean annual precipitation	1.88	0.82	-2.20E-04	-2.35	0.019	
	Mean annual temperature	0.74	0.72	0.01	2.30	0.022	
	NRI	0.12	1.00	-0.91	-4.31	< 0.001	

Table 3. Rates of transition (events per million years; from row to column) among the temperate and tropical regions of the Western Hemisphere. The highest rates (*) of transition occur between the tropical and southern temperate regions. The lowest rates of transition (ǂ) occur between the temperate zones.

	TR	NTR	STR
Tropical Range (TR)		61.98	156.05*
Northern temperate range (NTR)	57.36		16.01ǂ
Southern temperate range (STR)	119.40*	9.18ǂ	

Table S1. Model averaged coefficients (< 10 ΔAICc) and importance for all independent variables included in the study. We used generalized least squares models with a Gaussian spatial correlation structure. Model fit was evaluated using AICc. NRI is the Net Relatedness Index.

Region	Model terms	Model Averaged Coefficients	Importance
Tropics	Average C-score	1.60	1.00
	NRI	-0.25	1.00
	Mean annual precipitation	-2.30E-05	0.86
	Mean annual temperature	9.00E-04	0.35
	Species richness	-2.83E-03	1.00
Northern Temperate	Average C-score	0.75	1.00
	NRI	-1.00	1.00
	Mean annual precipitation	-2.59E-04	1.00
	Mean annual temperature	-0.02	1.00
	Species richness	-4.77E-03	0.98
Southern Temperate	Average C-score	0.22	0.33
	Mean annual precipitation	-2.20E-04	0.82
	NRI	-0.91	1.00
	Species richness	-4.79E-03	0.80
	Mean annual temperature	0.01	0.72
	Average C-score	0.22	0.33

Figure Captions

FIGURE 1. Phylogenetic maps of (A) ln transformed body masses of the smallest mammals in red and the largest in blue and (B) regions of occupancy including tropics (brown), northern temperate (red), and southern temperate (blue). Lighter shades of color indicate absence from a region. Per. and Artio. refer to the Perissodactyla and Artiodactyla, respectively.

FIGURE 2. Latitudinal patterns of (A) ln transformed body mass dispersion, (B) phylogenetic community structure measured using the Net Relatedness Index (NRI), and (C) average checkerboard or C-scores of Western Hemisphere mammal communities across tropical and temperate latitudes (demarcated by dashed lines). Communities were defined as species that co-occur in the same 100 km by 100 km grid cell laid over North, Central, and South America. Randomized communities are shown in gray in panel A. We used the independent swap algorithm of Gotelli (2000) to construct null models for the Net Relatedness Index.

FIGURE 3. Randomizations of body mass dispersion (BM_{dist}) and C-scores. (A) Standardized effects sizes for BM_{dist} (SES BM_{dist}) in each 100x100 km grid cell. (B) mean randomized C-scores (+/- standard deviation) per 100km by 100km grid cell, and (C) standardize effects sizes for C-scores in each 100km by 100km grid cell. Standardized effect sizes were calculated as SES = (obs – mean(random)) / sd(random). We did not calculate p-values nor rely on an arbitrary cut off for significance.

Figure 4. Relationship of mean body size differences among (A-B) tropical, (C-D), Northern Hemisphere, and (E-F) Southern Hemisphere mammals Western Hemisphere mammals with mean annual temperature (°C) and precipitation (mm), respectively.

FIGURE S1. Maps of (A) ln transformed body mass dispersion, (B) phylogenetic community structure measured using the Net Relatedness Index (NRI), and (C) average checkerboard or C-

scores of Western Hemisphere mammal communities across tropical and temperate latitudes (demarcated by dashed lines). Communities were defined as species that co-occur in the same 100 km by 100 km grid cell laid over North, Central, and South America. Randomized communities are shown in gray in panel A. We used the independent swap algorithm of Gotelli (2000) to construct null models for the Net Relatedness Index.

FIGURE S2. Maps of randomizations of body mass dispersion (BM_{dist}) and C-scores. (A) Standardized effects sizes for BM_{dist} (SES BM_{dist}) in each 100x100 km grid cell. (B) standardize effects sizes for C-scores in each 100km by 100km grid cell. Standardized effect sizes were calculated as SES = (obs – mean(random)) / sd(random). We did not calculate p-values nor rely on an arbitrary cut off for significance.

FIGURE S3. Latitudinal patterns of (A) ln transformed body mass differences, (B) phylogenetic community structure measured using the Net Relatedness Index (NRI), and (C) average checkerboard or C-scores of Western Hemisphere mammal communities across tropical and temperate latitudes (demarcated by dashed lines). Communities were defined as species that co-occur in the same 100 km by 100 km grid cell laid over North, Central, and South America. Randomized communities are shown in gray in panel A. For body mass dispersion, we used a null model wherein grid cell richness was maintained but not species occupancy. The regional pool from which species were drawn was limited to those present in the same biogeographic zone. For NRI, we used a null model wherein taxon labels were shuffled on the grid cell by species occurrence matrix (a similar method that also maintains site richness).

FIGURE S4. Latitudinal patterns of (A) ln transformed body mass differences, (B) phylogenetic community structure measured using the Net Relatedness Index (NRI), and (C) average checkerboard or C-scores of Western Hemisphere mammal communities across tropical and

temperate latitudes (demarcated by dashed lines). Species without body sized data were assigned a genus average body mass. Communities were defined as species the co-occur in the same 100 km by 100 km grid cell laid over North, Central, and South America. Randomized communities are shown in gray in panel A. We used the independent swap algorithm of Gotelli (2000) to construct null models for the Net Relatedness Index.

FIGURE S5. Latitudinal patterns of (A) ln transformed body mass differences, (B) phylogenetic community structure measured using the Net Relatedness Index (NRI), and (C) average checkerboard or C-scores of Western Hemisphere mammal communities across tropical and temperate latitudes (demarcated by dashed lines). Carnivorous species were excluded. Communities were defined as species the co-occur in the same 100 km by 100 km grid cell laid over North, Central, and South America. Randomized communities are shown in gray in panel A. We used the independent swap algorithm of Gotelli (2000) to construct null models for the Net Relatedness Index.

FIGURE S6. Latitudinal patterns of (A) ln transformed body mass differences, (B) phylogenetic community structure measured using the Net Relatedness Index (NRI), and (C) average checkerboard or C-scores of Western Hemisphere mammal communities across tropical and temperate latitudes (demarcated by dashed lines). Species without body sized data were assigned a genus average body mass. Communities were defined as species the co-occur in the same 50 km by 50 km grid cell laid over North, Central, and South America. Randomized communities are shown in gray in panel A. We used the independent swap algorithm of Gotelli (2000) to construct null models for the Net Relatedness Index.

FIGURE S7. Relationship of Western Hemisphere mammal assemblage-averaged species occupancy with (A) latitude (˚N) and (B) assemblage-averaged checkerboard or C-scores.

Communities were defined as species the co-occur in the same 100 km by 100 km grid cell laid over North, Central, and South America. Red points indicate grid cells that occur at the tropical-temperate transition zones, particularly between the tropics and Southern Temperate zone.

Figure. S8. Change in (A) mean annual temperatures (°C) and (B) mean annual precipitation (mm) with latitude in the Western Hemisphere. Data are from climatewizard.org.

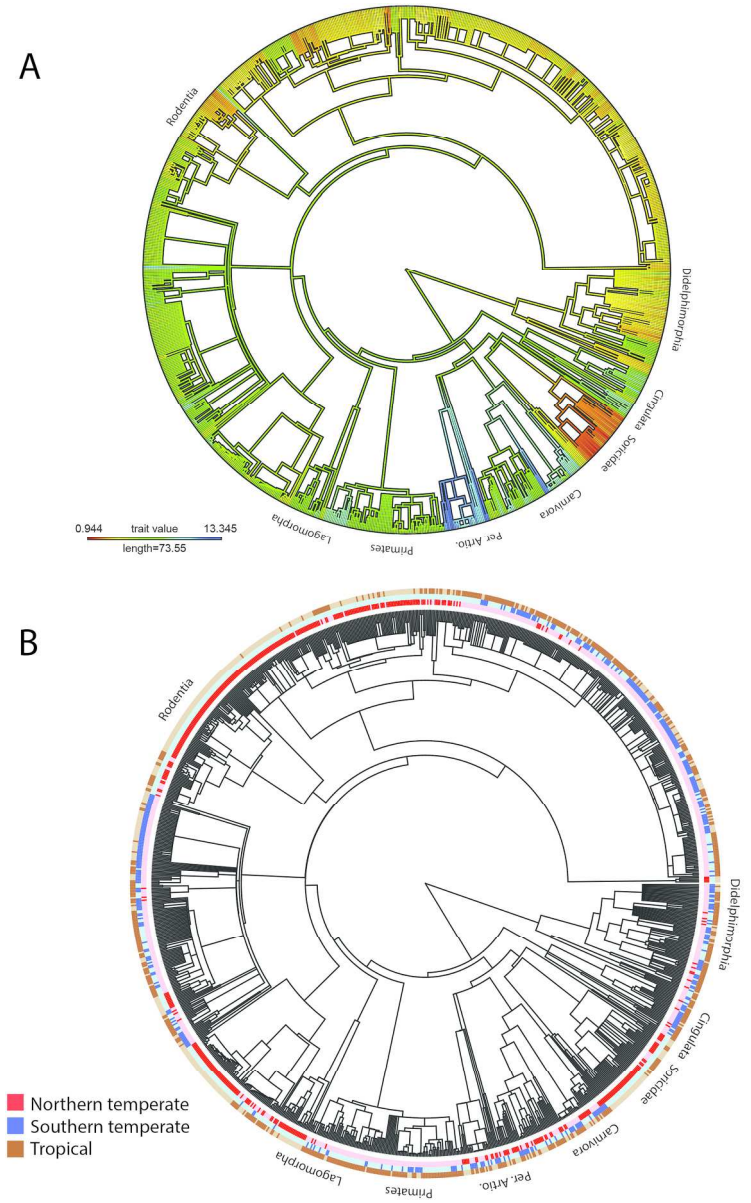

FIGURE 1. Phylogenetic maps of (A) ln transformed body masses of the smallest mammals in red and the largest in blue and (B) regions of occupancy including tropics (brown), northern temperate (red), and southern temperate (blue). Lighter shades of color indicate absence from a region. Per. and Artio. refer to the Perissodactyla and Artiodactyla, respectively.

178x289mm (300 x 300 DPI)

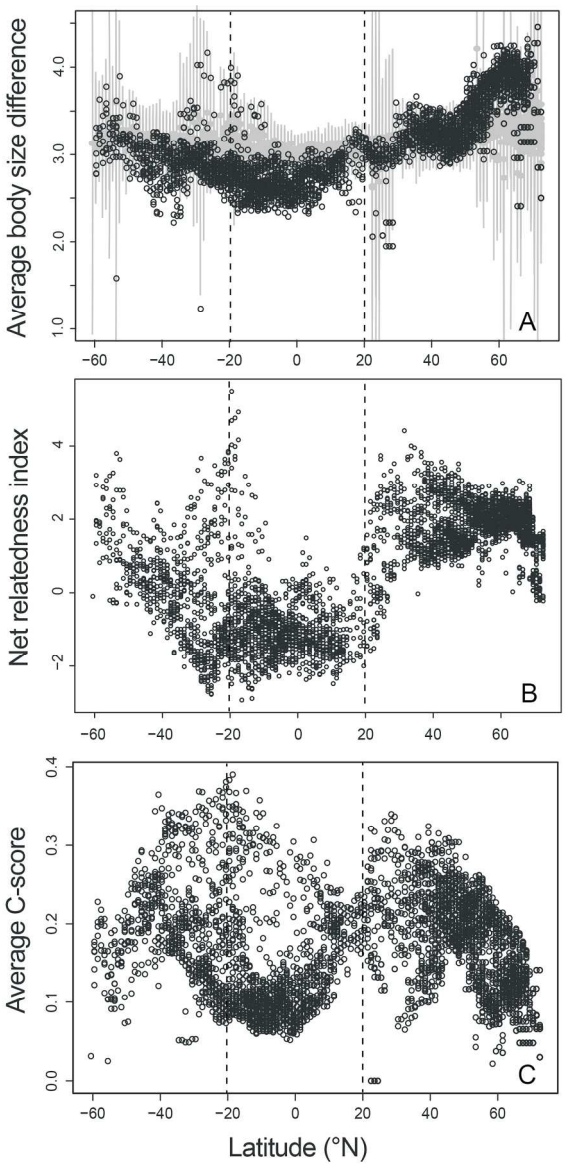

FIGURE 2. Latitudinal patterns of (A) ln transformed body mass dispersion, (B) phylogenetic community structure measured using the Net Relatedness Index (NRI), and (C) average checkerboard or C-scores of Western Hemisphere mammal communities across tropical and temperate latitudes (demarcated by dashed lines). Communities were defined as species that co-occur in the same 100 km by 100 km grid cell laid over North, Central, and South America. Randomized communities are shown in gray in panel A. We used the independent swap algorithm of Gotelli (2000) to construct null models for the Net Relatedness Index.

160x324mm (300 x 300 DPI)

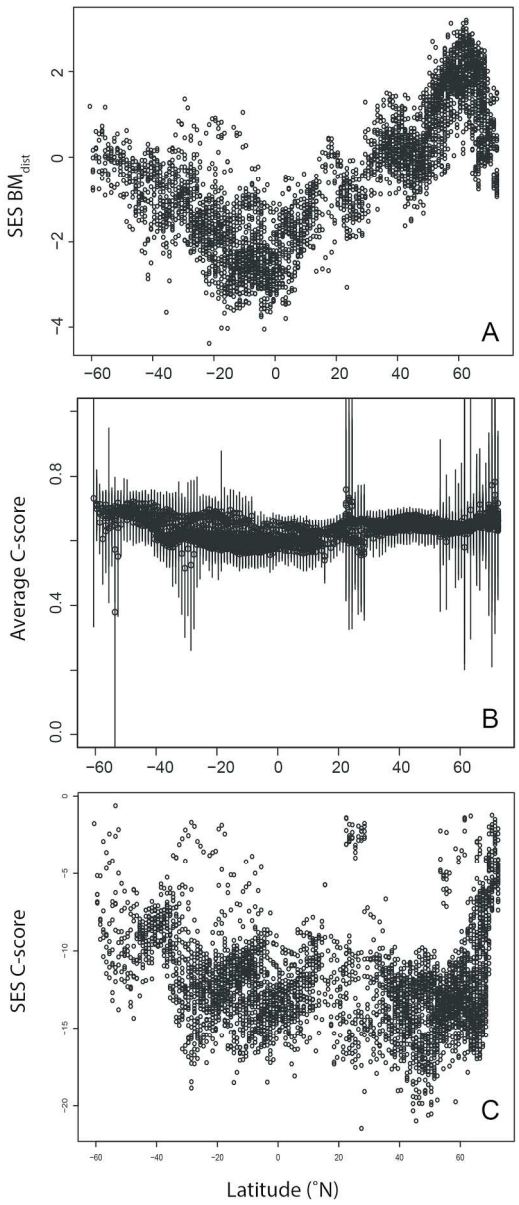

FIGURE 3. Randomizations of body mass dispersion (BMdist) and C-scores. (A) Standardized effects sizes for BMdist (SES BMdist) in each 100x100 km grid cell. (B) mean randomized C-scores (+/- standard deviation) per 100km by 100km grid cell, and (C) standardize effects sizes for C-scores in each 100km by 100km grid cell. Standardized effect sizes were calculated as SES = (obs – mean(random)) / sd(random). We did not calculate p-values nor rely on an arbitrary cut off for significance.

172x378mm (300 x 300 DPI)

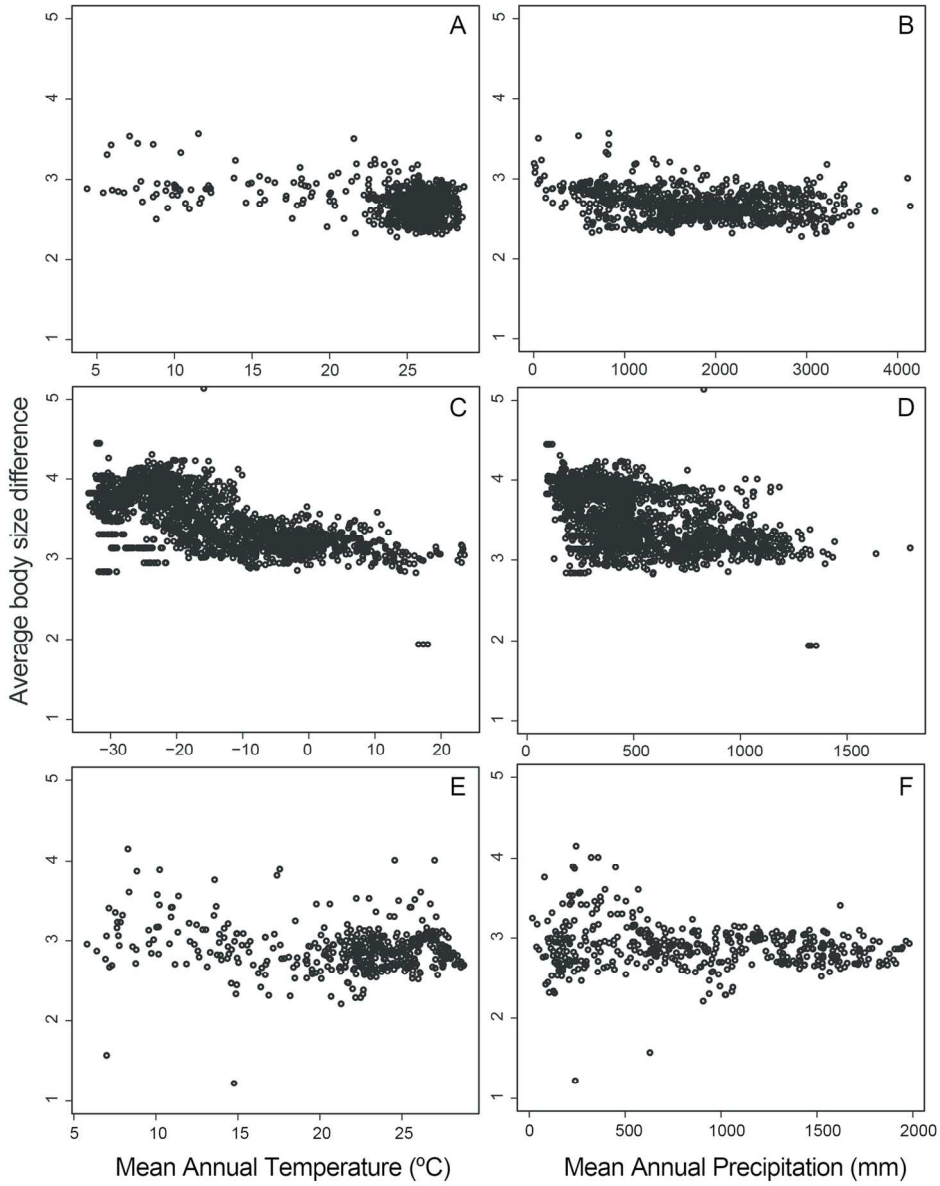

Figure 4. Relationship of mean body size differences among (A-B) tropical, (C-D), Northern Hemisphere, and (E-F) Southern Hemisphere mammals Western Hemisphere mammals with mean annual temperature (°C) and precipitation (mm), respectively.

138x175mm (300 x 300 DPI)

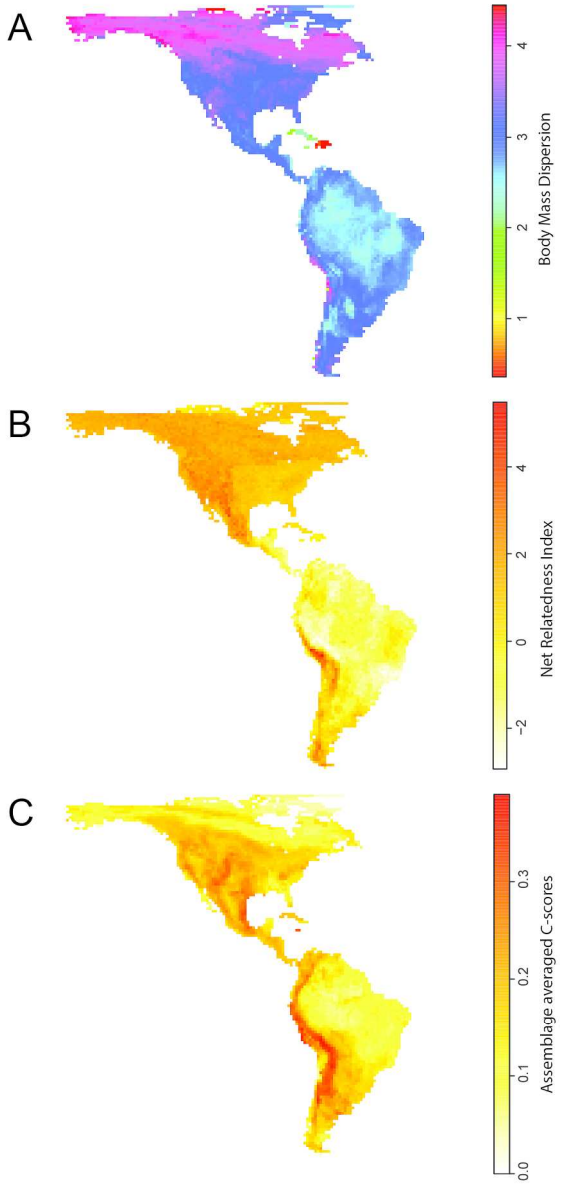

FIGURE S1. Maps of (A) ln transformed body mass dispersion, (B) phylogenetic community structure measured using the Net Relatedness Index (NRI), and (C) average checkerboard or C-scores of Western Hemisphere mammal communities across tropical and temperate latitudes (demarcated by dashed lines). Communities were defined as species that co-occur in the same 100 km by 100 km grid cell laid over North, Central, and South America. Randomized communities are shown in gray in panel A. We used the independent swap algorithm of Gotelli (2000) to construct null models for the Net Relatedness Index.

342x698mm (300 x 300 DPI)

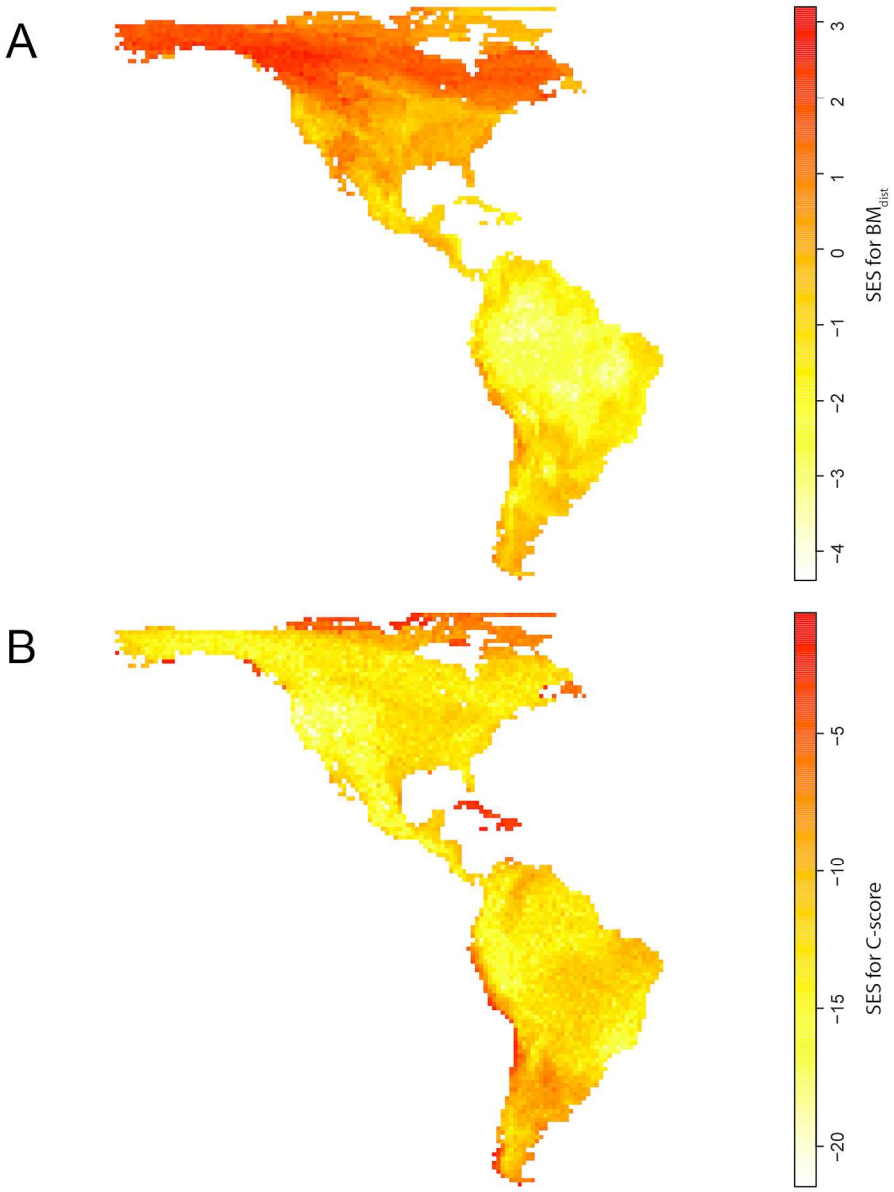

FIGURE S2. Maps of randomizations of body mass dispersion (BMdist) and C-scores. (A) Standardized effects sizes for BMdist (SES BMdist) in each 100x100 km grid cell. (B) standardize effects sizes for C-scores in each 100km by 100km grid cell. Standardized effect sizes were calculated as SES = (obs – mean(random)) / sd(random). We did not calculate p-values nor rely on an arbitrary cut off for significance.

218x283mm (300 x 300 DPI)

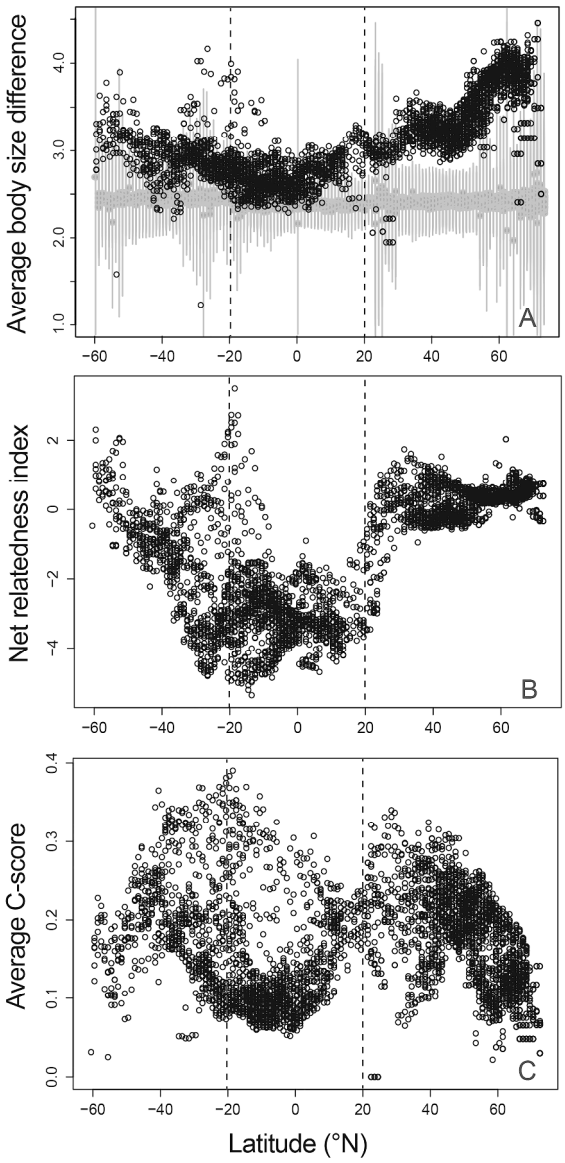

FIGURE S3. Latitudinal patterns of (A) ln transformed body mass differences, (B) phylogenetic community structure measured using the Net Relatedness Index (NRI), and (C) average checkerboard or C-scores of Western Hemisphere mammal communities across tropical and temperate latitudes (demarcated by dashed lines). Communities were defined as species that co-occur in the same 100 km by 100 km grid cell laid over North, Central, and South America. Randomized communities are shown in gray in panel A. For body mass dispersion, we used a null model wherein grid cell richness was maintained but not species occupancy. The regional pool from which species were drawn was limited to those present in the same biogeographic zone. For NRI, we used a null model wherein taxon labels were shuffled on the grid cell by species occurrence matrix (a similar method that also maintains site richness).

340x690mm (300 x 300 DPI)

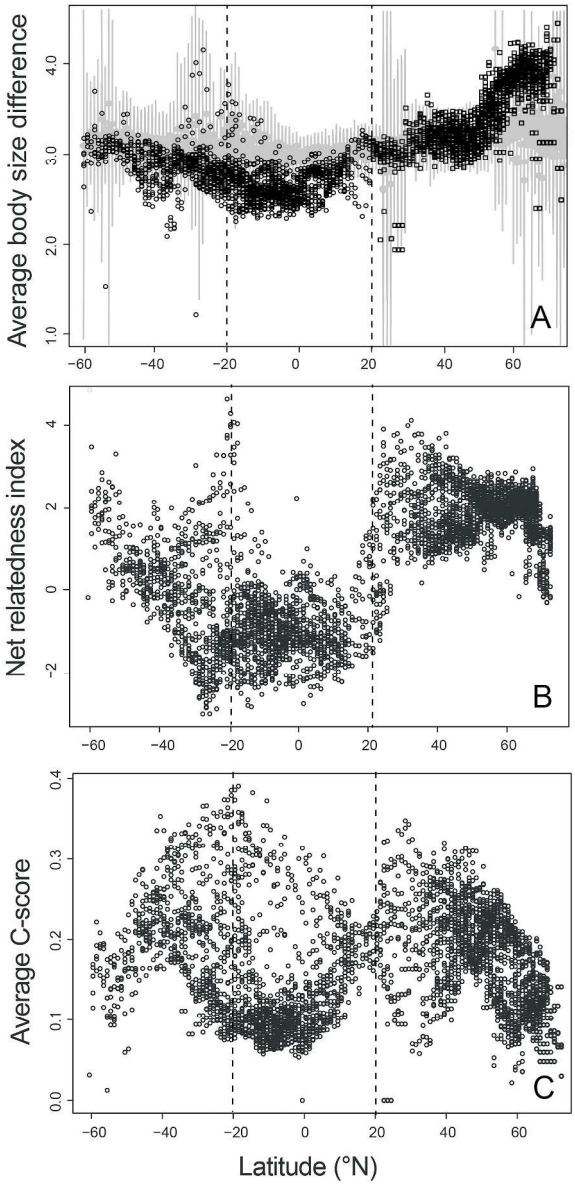

FIGURE S4. Latitudinal patterns of (A) ln transformed body mass differences, (B) phylogenetic community structure measured using the Net Relatedness Index (NRI), and (C) average checkerboard or C-scores of Western Hemisphere mammal communities across tropical and temperate latitudes (demarcated by dashed lines). Species without body sized data were assigned a genus average body mass. Communities were defined as species the co-occur in the same 100 km by 100 km grid cell laid over North, Central, and South America. Randomized communities are shown in gray in panel A. We used the independent swap algorithm of Gotelli (2000) to construct null models for the Net Relatedness Index.

327x639mm (300 x 300 DPI)

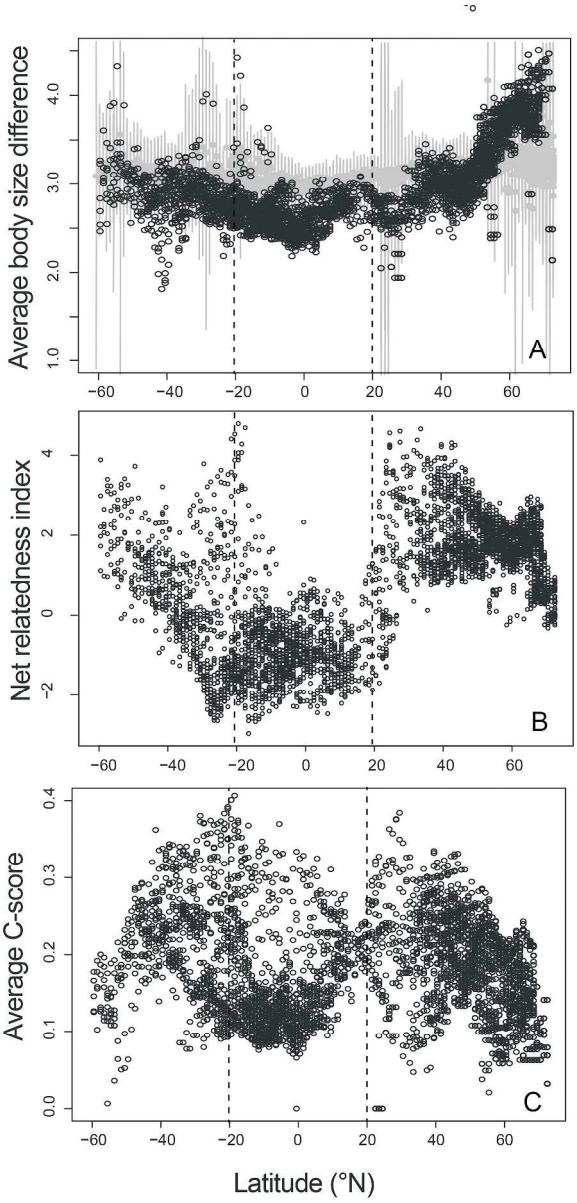

FIGURE S5. Latitudinal patterns of (A) ln transformed body mass differences, (B) phylogenetic community structure measured using the Net Relatedness Index (NRI), and (C) average checkerboard or C-scores of Western Hemisphere mammal communities across tropical and temperate latitudes (demarcated by dashed lines). Carnivorous species were excluded. Communities were defined as species the co-occur in the same 100 km by 100 km grid cell laid over North, Central, and South America. Randomized communities are shown in gray in panel A. We used the independent swap algorithm of Gotelli (2000) to construct null models for the Net Relatedness Index.

333x661mm (300 x 300 DPI)

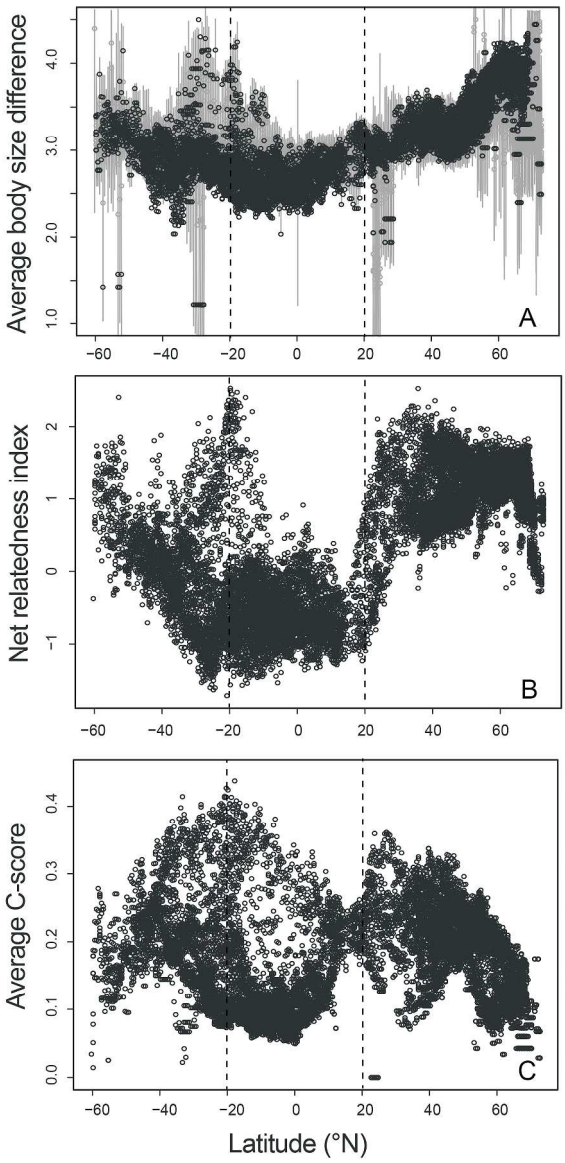

FIGURE S6. Latitudinal patterns of (A) ln transformed body mass differences, (B) phylogenetic community structure measured using the Net Relatedness Index (NRI), and (C) average checkerboard or C-scores of Western Hemisphere mammal communities across tropical and temperate latitudes (demarcated by dashed lines). Species without body sized data were assigned a genus average body mass. Communities were defined as species the co-occur in the same 50 km by 50 km grid cell laid over North, Central, and South America. Randomized communities are shown in gray in panel A. We used the independent swap algorithm of Gotelli (2000) to construct null models for the Net Relatedness Index.

340x690mm (300 x 300 DPI)

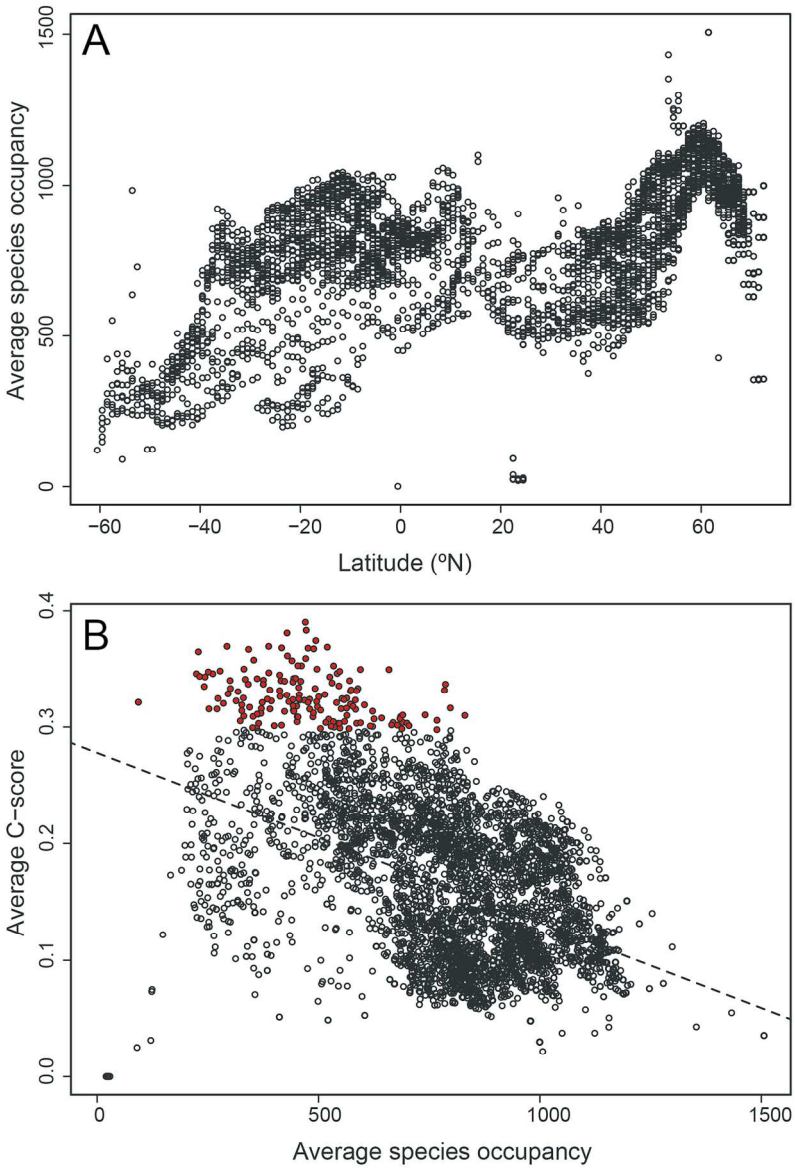

FIGURE S7. Relationship of Western Hemisphere mammal assemblage-averaged species occupancy with (A) latitude (˚N) and (B) assemblage-averaged checkerboard or C-scores. Communities were defined as species the co-occur in the same 100 km by 100 km grid cell laid over North, Central, and South America. Red points indicate grid cells that occur at the tropical-temperate transition zones, particularly between the tropics and Southern Temperate zone.

158x227mm (300 x 300 DPI)

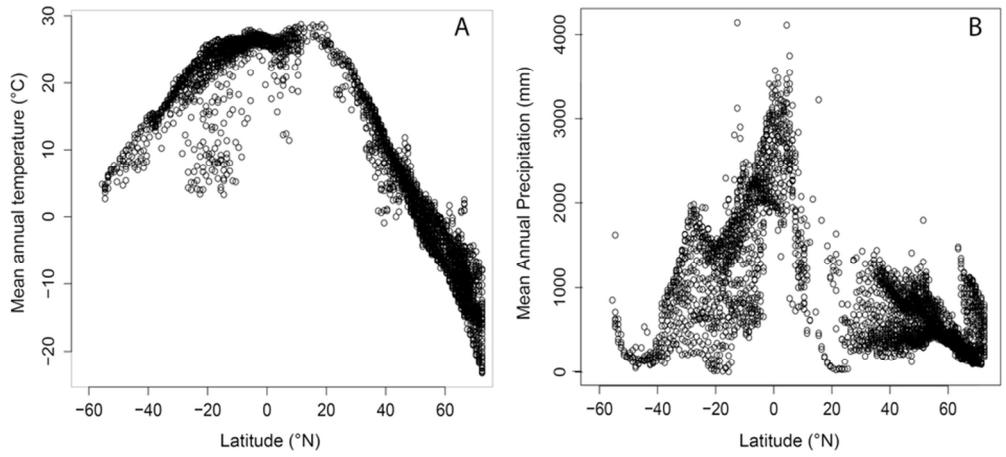

Figure. S8. Change in (A) mean annual temperatures (°C) and (B) mean annual precipitation (mm) with latitude in the Western Hemisphere. Data are from climatewizard.org.

81x39mm (300 x 300 DPI)